UC Davis
UC Davis Previously Published Works

Title

Trp triad-dependent rapid photoreduction is not required for the function of Arabidopsis CRY1

Permalink

https://escholarship.org/uc/item/8bm8f9zg

Journal

Proceedings of the National Academy of Sciences of the United States of America, 112(29)

ISSN

0027-8424

Authors

Gao, Jie
Wang, Xu
Zhang, Meng
et al.

Publication Date

2015-07-21

DOI

10.1073/pnas.1504404112

Peer reviewed

Trp triad-dependent rapid photoreduction is not required for the function of *Arabidopsis* CRY1

Jie Gao[a,b,1], Xu Wang[b,c,1], Meng Zhang[d,e,1], Mingdi Bian[a,1], Weixian Deng[a], Zecheng Zuo[a], Zhenming Yang[a,2], Dongping Zhong[d,e,2], and Chentao Lin[b,2]

[a]Laboratory of Soil and Plant Molecular Genetics, College of Plant Science, Jilin University, Changchun 130062, China; [b]Department of Molecular, Cell and Developmental Biology, University of California, Los Angeles, CA 90095; [c]Basic Forestry and Proteomics Research Center, Fujian Agriculture and Forestry University, Fuzhou 350002, China; [d]Department of Physics, Ohio State University, Columbus, OH 43210; and [e]Department of Chemistry and Biochemistry, Ohio State University, Columbus, OH 43210

Cryptochromes in different evolutionary lineages act as either photoreceptors or light-independent transcription repressors. The flavin cofactor of both types of cryptochromes can be photoreduced in vitro by electron transportation via three evolutionarily conserved tryptophan residues known as the "Trp triad." It was hypothesized that Trp triad-dependent photoreduction leads directly to photoexcitation of cryptochrome photoreceptors. We tested this hypothesis by analyzing mutations of *Arabidopsis* cryptochrome 1 (CRY1) altered in each of the three Trp-triad tryptophan residues (W324, W377, and W400). Surprisingly, in contrast to a previous report all photoreduction-deficient Trp-triad mutations of CRY1 remained physiologically and biochemically active in *Arabidopsis* plants. ATP did not enhance rapid photoreduction of the wild-type CRY1, nor did it rescue the defective photoreduction of the CRY1^{W324A} and CRY1^{W400F} mutants that are photophysiologically active in vivo. The lack of correlation between rapid flavin photoreduction or the effect of ATP on the rapid flavin photoreduction and the in vivo photophysiological activities of plant cryptochromes argues that the Trp triad-dependent photoreduction is not required for the function of cryptochromes and that further efforts are needed to elucidate the photoexcitation mechanism of cryptochrome photoreceptors.

cryptochrome | blue light | *Arabidopsis* | Trp-triad | photoreduction

How chemical or physical properties of proteins observed in vitro are associated with their functions in vivo is often a challenging question in biology. For example, free flavins and flavin cofactors of flavoproteins commonly undergo photoreduction in vitro, whereby oxidized flavins are converted to a reduced form upon exposure to light, although few of those "photoreducible" flavoproteins, such as D-amino acid oxidase and glucose oxidase, possess light-dependent functions in vivo (1, 2). Cryptochromes are photolyase-like flavoproteins that act as photoreceptors regulating light responses in plants and *Drosophila* or as light-independent transcription repressors of the circadian clock in mammals (3–6). Like other flavoproteins, cryptochromes can be photoreduced in vitro regardless of their photobiological activity in vivo (7–10). There are five evolutionarily conserved tryptophan residues within a region associated with the flavin adenine dinucleotide (FAD)-binding pocket of the photolyase-homologous region (PHR) domain of cryptochromes (Fig. 1*A*). Three of those five tryptophan residues, referred to as the "Trp triad," are required for the in vitro photoreduction of cryptochromes (8, 11–13). Photoreduction of cryptochromes has been studied extensively and is widely accepted as the photoexcitation mechanism of cryptochrome photoreceptors (6).

Most evidence supporting the photoreduction hypothesis came from in vitro biophysical studies (6, 14). The only genetics study reported so far in support of the hypothesis that Trp triad-dependent photoreduction is required for the physiological activities of cryptochrome photoreceptors came from a study of *Arabidopsis* cryptochrome 1 (CRY1) (15). It was reported that

mutations in two of the three Trp-triad residues of *Arabidopsis* CRY1—W324 and W400—abolished or dramatically reduced the photophysiological activities of CRY1 in transgenic plants (15). In contrast, all other genetics studies reported to date showed that mutations at the Trp-triad residues of the photolyase/cryptochrome proteins do not significantly affect the in vivo activity of the respective mutants. For example, Trp triad-dependent photoreduction is not required for the in vivo DNA-repairing activity of *Escherichia coli* photolyase (16–18), the photobiochemical and magnetosensing activities of *Drosophila* cryptochrome (10, 13, 19–21), or the photobiochemical and photophysiological activities of *Arabidopsis* CRY2 (22). It was proposed recently that ATP or other metabolites may enhance the rapid photoreduction of CRY2 to "rescue" its defects in photoreduction and physiological activities in vivo (23). However, because Trp-triad mutations were reported to inactivate CRY1 (15) but not CRY2 in vivo (22), this interpretation raises the intriguing possibility that *Arabidopsis* CRY1 might possess a photoexcitation mechanism distinct from both the closely related *Arabidopsis* CRY2 and the remotely related *E. coli* photolyase and *Drosophila* cryptochrome. To investigate this puzzle and the photoactivation mechanism of cryptochromes in general, we analyzed the Trp-triad mutants of CRY1, including the previously reported mutants W324 and W400 (15), to test whether photoreduction or ATP enhancement of photoreduction is required for the function of CRY1.

Significance

The Trp triad-dependent photoreduction of the flavin chromophore has been widely accepted as the photoexcitation mechanism of cryptochrome photoreceptors. However, the experimental evidence supporting this hypothesis derived primarily from the biophysical studies in vitro, except for one genetics study of *Arabidopsis* cryptochrome 1 (CRY1). In contrast to the previous report, we found that all Trp-triad mutations of *Arabidopsis* CRY1 remained physiologically active in plants, and this result cannot be readily explained by the ATP-dependent enhancement of Trp triad-dependent photoreduction. Our results challenge the widely accepted Trp-triad hypothesis and call for further investigation of alternative electron transport mechanisms to explain cryptochrome photoexcitation.

Fig. 1. The Trp triad-dependent photoreduction of *Arabidopsis* CRY1. (*A*) The structure of CRY1 (Protein Data Bank ID code 1U3C) showing the Trp-triad residues W324, W377, and W400. FAD (orange), the Trp-triad tryptophan residues (blue), and two evolutionarily conserved non–Trp-triad tryptophan residues (green) are indicated. (*B*) Sequence alignment of the Trp-triad region of a *Synechococcus elongates* photolyase (SePhr), *E. coli* photolyase (EcPhr), *Drosophila* cryptochrome (DmRY), human CRY1 and CRY2 (HsCRY1, HsCRY2), and *Arabidopsis* CRY1 and CRY2 (AtCRY1, AtCRY2). The Trp-triad residues (blue) and the other two conserved non–Trp-triad tryptophan residues (green) are indicated. The positions of the five conserved tryptophan residues in AtCRY1 are labeled at the bottom. The alignment was generated by ClustalX and modified by Genedoc. (*C–N*) Photoreduction of the wild-type CRY1 and the indicated CRY1 mutant proteins expressed and purified from Sf9 insect cells is shown. The scanning absorption spectra (*C–E* and *I–K*) were recorded after blue light (450 ± 15 nm, 1.8 mW/cm², or 70 μmol·m⁻²·s⁻¹) treatment for 10 min in the absence (B10) or presence of 1 mM ATP [B10 (+ATP)] under anaerobic conditions at 20 °C, in the presence of 10 mM β-mercaptoethanol as external electron donor. The difference spectra of indicated proteins are shown in *F–H* and *L–N*. a.u., arbitrary units.

Results

Lack of Correlation Between ATP-Enhanced Photoreduction and Trp Triad-Dependent Photoreduction of CRY1.

Five tryptophan residues in the PHR domain of *Arabidopsis* CRY1—the Trp-triad residues W324, W377, and W400 and two non–Trp-triad residues, W334 and W356—are evolutionarily conserved in the photolyase/cryptochrome proteins (Fig. 1 *A* and *B*) (24). We prepared site-specific mutations by individually replacing each of the five conserved

tryptophan residues with either alanine or phenylalanine that is redox inert but structurally more similar to tryptophan than alanine, using the site-directed mutagenesis method. These CRY1 mutations are referred to as "CRY1^{W324A}" (W324A), "CRY1^{W324F}" (W324F), "CRY1^{W377A}" (W377A), "CRY1^{W377F}" (W377F), "CRY1^{W400A}" (W400A), "CRY1^{W400F}" (W400F), "CRY1^{W334A}" (W334A), "CRY1^{W334F}" (W334F), "CRY1^{W356A}" (W356A), and "CRY1^{W356F}" (W356F). Eight of the ten His-tagged CRY1 recombinant proteins (all except W334A and W400A) were expressed successfully and purified from insect cells (Fig. 1 and *SI Appendix,* Fig. S1). As expected, the wild-type CRY1 protein showed a rapid (within 10 min) photoreduction in vitro under anaerobic conditions, as reported previously (Fig. 1*C*) (7). Mutations of any Trp-triad tryptophan residues (W400, W377, or W324) by either alanine or phenylalanine abolished or dramatically reduced the rapid photoreduction activity of the respective mutant CRY1 protein (Fig. 1 *C–N*). In contrast, mutations of the other two evolutionarily conserved tryptophan residues, W334 and W356, showed rapid photoreduction activity similar to that of the wild-type CRY1 protein (*SI Appendix,* Fig. S1). These results confirmed that only the Trp-triad residues are required for the rapid in vitro photoreduction of *Arabidopsis* CRY1.

It is well known that flavins and flavoproteins are photoreducible in vitro and that many small molecules, such as EDTA, urea, flavin, NADH, and amino acids, can enhance in vitro flavin photoreduction (1, 2, 25–27). It has been reported recently that metabolites such as ATP or NADH enhance photoreduction of *Arabidopsis* CRY2 (23), suggesting a compelling explanation of why the Trp-triad mutations of *Arabidopsis* CRY2 that do not undergo photoreduction in vitro are photophysiologically active in vivo. ATP-enhanced photoreduction also has been reported for the PHR domain of CRY1 (28, 29), supporting the hypothesis that metabolites such as ATP may act as regulators of cryptochromes in cells. We tested this hypothesis by investigating whether ATP may enhance photoreduction of *Arabidopsis* CRY1 and whether ATP may rescue the defective photoreduction of the Trp-triad mutants of CRY1. In contrast to the full-length CRY2 or truncated CRY1, ATP failed to enhance the rapid photoreduction of the full-length *Arabidopsis* CRY1 under conditions similar to those reported previously for CRY2 (Fig. 1 *C* and *F* and *SI Appendix,* Fig. S2). Importantly, ATP also failed to rescue the defective photoreduction of the Trp-triad mutant W400F of CRY1 (Fig. 1 *D* and *G* and *SI Appendix,* Fig. S2) and even slightly inhibited the residual photoreduction of the Trp-triad mutant W324A (Fig. 1 *E* and *H* and *SI Appendix,* Fig. S3). ATP did enhance photoreduction of other Trp-triad mutants of CRY1 (W324F, W377A, and W377F) that are defective in photoreduction. ATP also accelerated or enhanced photoreduction of the non–Trp-triad CRY1 mutation W334F and W356F that showed no apparent defect in photoreduction (Fig. 1 and *SI Appendix,* Figs. S1–S5). If the in vivo activity of Trp-triad mutants was caused by ATP-enhanced photoreduction, ATP would be expected to rescue light-dependent flavin reduction of the Trp-triad mutants that possess light-dependent physiological activities in vivo and to exert light-independent enhancement of flavin reduction of the Trp-triad mutants that exhibit light-independent or constitutive activities in vivo. In contrast to both expectations, it had been reported previously that ATP enhanced light-dependent flavin reduction or photoreduction of the W374A mutant of CRY2 that is constitutively active in vivo (22, 23) but failed to enhance photoreduction of the W397F mutant of CRY2 that showed light-dependent activities in plants (22, 23). Similarly, ATP failed to enhance photoreduction of the W324A and W400F mutants of CRY1 (Fig. 1), both of which exhibit light-dependent physiological activities in plants (see below). Taken together, these results demonstrate a lack of correlation between the ATP-enhanced photoreduction and light-dependent functions of CRY1 and CRY2.

Trp Triad-Dependent Photoreduction Is Not Required for the Photophysiological Activities of CRY1. CRY1 mediates blue light inhibition of hypocotyl growth, blue light stimulation of anthocyanin accumulation, and blue light induction of mRNA expression (30–33). To test the photophysiological activities of the Trp-triad mutants of CRY1, we prepared transgenic *Arabidopsis* lines expressing wild-type or mutant CRY1 as the GFP-CRY1 fusion proteins under the control of the constitutive 35S promoter in the *cry1* mutant background. For simplicity, the different GFP-CRY1 fusion proteins (GFP-CRY1, GFP-CRY1^{W324A}, GFP-CRY1^{W324F}, GFP-CRY1^{W377A}, GFP-CRY1^{W377F}, GFP-CRY1^{W400A}, and GFP-CRY1^{W400F}, GFP-CRY1^{W334A}, GFP-CRY1^{W334F}, GFP-CRY1^{W356A}, GFP-CRY1^{W356F}) are referred to hereafter as "CRY1," "W324A," "W324F," "W377A," "W377F," "W400A," "W400F," "W334A," "W334F," "W356A," and "W356F," respectively. All CRY1 mutant proteins accumulated in the nucleus and cytoplasm as the wild-type CRY1 control (*SI Appendix*, Figs. S6 and S7) (34). To ensure that the observed physiological activities of the Trp-triad mutants of CRY1 are not caused by higher levels of protein expression, transgenic lines expressing the mutant CRY1 proteins at the levels similar to or slightly lower than that of the wild-type GFP-CRY1 control (Fig. 2 *A* and *B* and *SI Appendix*, Fig. S8 *A* and *B* and Table S1) were selected for phenotypic studies. The genotypes of the transgenic lines used for detailed phenotypic analyses (*SI Appendix*, Fig. S6*A*) were verified by genomic sequencing, and the hypocotyl inhibition activity of all transgenes was confirmed in three independent lines (*SI Appendix*, Figs. S9 and S10). The overall results are summarized in *SI Appendix*, Table S1.

Surprisingly, in contrast to a previous report (15), none of the Trp-triad mutations of CRY1 abolished physiological activity inhibiting hypocotyl elongation (Fig. 2 *C* and *D* and *SI Appendix*, Figs. S8–S10). It was reported previously that mutations of the W324 or W400 residue of CRY1 were inactive in mediating blue light inhibition of hypocotyl elongation (15). However, in our experiment, mutations in all Trp-triad residues of CRY1, including W324 and W400, remained active in mediating blue light inhibition of hypocotyl elongation (Fig. 2). For example, the W324F and W324A mutants of CRY1 fully rescued the long hypocotyl phenotype of the *cry1* parent (Fig. 2 *C* and *D* and *SI Appendix*, Fig. S8 *C* and *D*). Transgenic seedlings expressing the W324F or W324A mutant developed hypocotyls as short as those expressing the wild-type GFP-CRY1 control when grown in continuous blue light (Fig. 2 *C* and *D* and *SI Appendix*, Fig. S8 *C* and *D*). The specific activity of the W324F and W324A mutants is comparable to or higher than that of the wild-type GFP-CRY1 control, because the protein level of the W324A or W324F mutants was about 60–70% that of the GFP-CRY1 control (*SI Appendix*, Table S1). Among the six Trp-triad mutants of CRY1 examined, four (W324A, W324F, W377F, and W400F) showed blue light-specific activity in growth inhibition (Fig. 2*D* and *SI Appendix*, Fig. S8*D*), whereas two mutants (W377A and W400A) exhibited activity stronger than that of the wild-type GFP-CRY1 control in growth inhibition without the blue light specificity (*SI Appendix*, Fig. S8 *C* and *D*). Seedlings expressing W377A showed light-dependent hypocotyl inhibition in both blue light and red light, whereas seedlings expressing W400A exhibited constitutive growth inhibition in both dark and light (*SI Appendix*, Fig. S8), a finding that is reminiscent of the W374A and W374F mutants of *Arabidopsis* CRY2 (22).

To measure the photophysiological activity of the Trp-triad mutants of CRY1 more accurately, we performed a fluence rate response analysis (*SI Appendix*, Fig. S11). In this experiment, the hypocotyl lengths of seedlings expressing each of the Trp-triad mutants of CRY1 were compared with the hypocotyl length of the parent *cry1* mutant (*cry1*), the wild type, and the transgenic line expressing the wild-type GFP-CRY1 control (CRY1) (*SI Appendix*, Fig. S11). *SI Appendix*, Fig. S11 shows that the apparent growth inhibition activity of the six Trp-triad mutants of
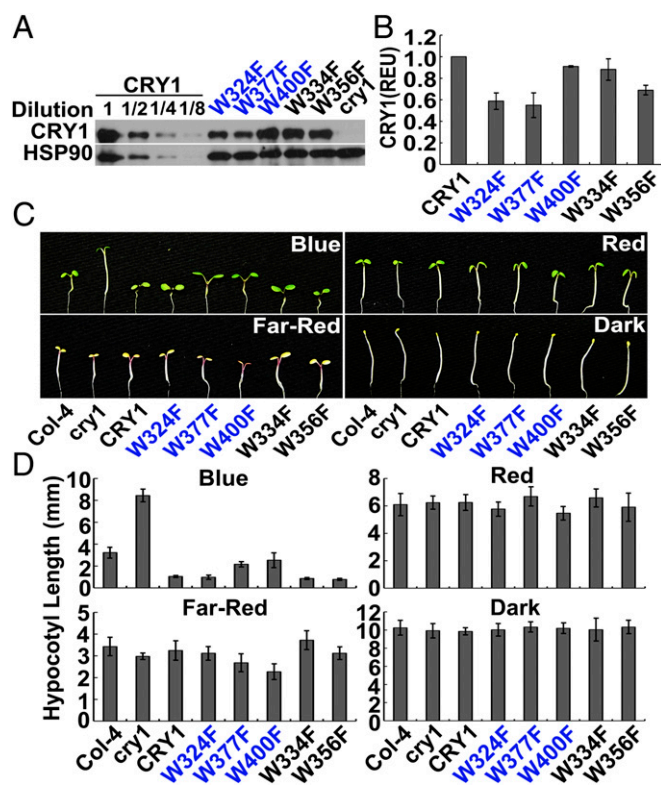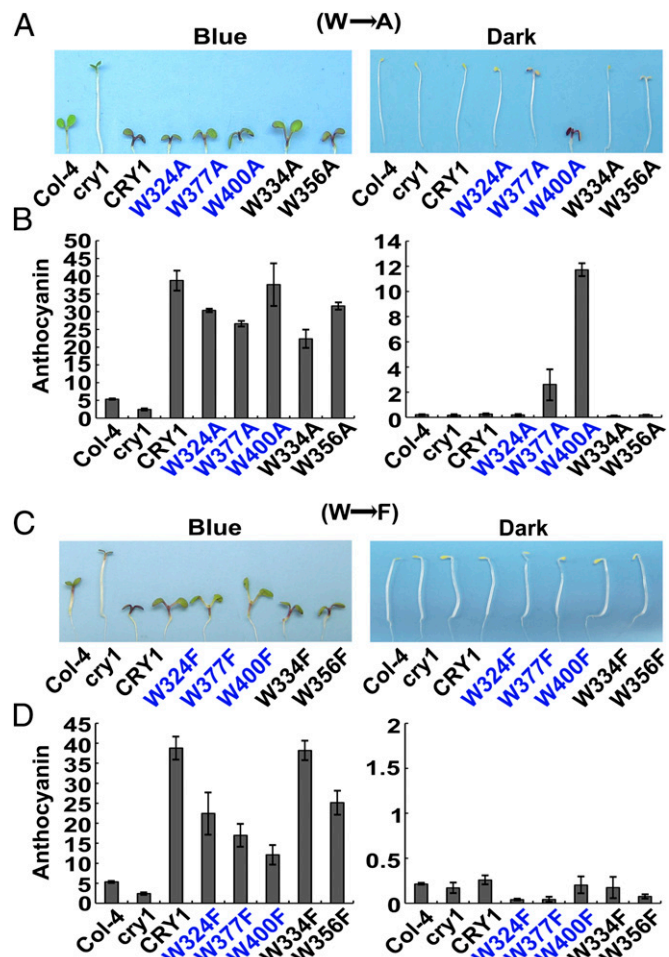

Fig. 2. The Trp-triad mutants of CRY1 are physiologically active in mediating blue light inhibition of hypocotyl elongation. (*A*) Immunoblot showing GFP-fusion proteins of the Trp triad (labeled in blue) and non–Trp-triad mutants of CRY1 expressed in transgenic plants. All transgenic lines are in the *cry1* background. Samples were extracted from seedlings grown on MS medium under continuous white light, fractionated in SDS/PAGE (10%), blotted, probed with anti-CRY1 antibody (CRY1), stripped, and reprobed with anti-HSP90 antibody (HSP90; Santa Cruz Biotechnology) as the loading control. A series dilution of the sample prepared from plants expressing the GFP-CRY1 control (CRY1) and the parental *cry1* mutant (*cry1*) are included to facilitate semiquantification. (*B*) The relative expression unit (REU) showing the semiquantification of the indicated proteins was calculated by the formula (CRY1^{mt}/HSP90^{mt})/(CRY1^{wt}/HSP90^{wt}). The CRY1 and HSP90 signals of the mutant (mt) and wild-type GFP-CRY1 (wt) samples were digitized and quantified by ImageJ. (*C*) Images showing representative seedlings of the indicated genotypes. Seedlings were grown on MS medium under continuous blue light (20 μmol·m^{-2}·s^{-1}), red light (18 μmol·m^{-2}·s^{-1}), far-red light (1.5 μmol·m^{-2}·s^{-1}), or in darkness for 5 d. (*D*) Hypocotyl lengths of indicated genotypes grown under the conditions in C were measured ($n \geq 20$). The wild-type plants (Col-4), the *cry1* mutant parent (*cry1*), and transgenic plants expressing the wild-type GFP-CRY1 (CRY1) controls are included. Error bars indicate SD.

CRY1 can be ranked in the following order in comparison with the wild-type GFP-CRY1 control: W400A > W377A > W324A ~ W324F ~ CRY1 > W377F ~ W400F. Taking into consideration the level of relative protein expression, we found that four (W400A, W377A, W324A, and W324F) of the six Trp-triad mutants tested exhibited apparent specific activities similar to or higher than that of the wild-type GFP-CRY1 control. For example, hypocotyl length in seedlings expressing W324A was indistinguishable from that of seedlings expressing the wild-type GFP-CRY1 control, although the level of relative protein expression in W324A is about 70% that of the GFP-CRY1 control (*SI Appendix*, Fig. S11 and Table S1). This result demonstrates that the photophysiological activity of W324A is at least similar to that of the wild-type CRY1. Seedlings expressing the W400A mutant (and to a lesser extent the W377A mutant) showed a constitutive photomorphogenic phenotype (*SI Appendix*, Fig. S11) that is reminiscent of the W374A mutant of CRY2 (22).

It is noteworthy that the constitutively active W400A mutation of CRY1 affects the Trp-triad residue (W400) that is the most proximate to FAD, whereas the constitutively active W374A mutation of CRY2 affects the Trp-triad residue (W374) located in the middle of the Trp triad. It also is interesting that both the W374F and W374A mutants of CRY2 are constitutively active (22), whereas only the W400A mutant but not the W400F mutant of CRY1 showed constitutive activities (Fig. 2 and *SI Appendix,* Figs. S8 and S11). Because (*i*) all Trp-triad mutants tested were able to rescue the *cry1* mutant (Fig. 2 and *SI Appendix,* Fig. S8), (*ii*) more than half of the six Trp-triad mutants tested exhibited specific activity similar to or higher than that of the GFP-CRY1 control (*SI Appendix,* Fig. S11 and Table S1), and (*iii*) ATP failed to enhance photoreduction of the wild-type CRY1 or to rescue the defective photoreduction of at least two Trp-triad mutants of CRY1 that are photophysiologically active in plants (Fig. 1 *C–E*), we propose that Trp triad-dependent photoreduction is not required for the photophysiological activity of CRY1.

To test this proposition further, we examined whether the Trp-triad mutants can mediate the blue light-induced anthocyanin accumulation and changes of gene expression in plants. Again, in contrast to the previous report (15), all Trp-triad mutants of CRY1 were able to mediate blue light stimulation of anthocyanin accumulation (Fig. 3). As shown in Fig. 3, transgenic plants expressing all six Trp-triad mutant proteins of CRY1 accumulated significantly higher ($P < 0.01$) levels of anthocyanin than the *cry1* mutant parent or the wild-type plants when grown in continuous blue light. Interestingly, the W-to-A Trp-triad mutants appear to exhibit higher activity than the W-to-F mutants of the same Trp-triad residues in both anthocyanin accumulation and hypocotyl inhibition responses (Fig. 3 and *SI Appendix,* Fig. S11). Because the phenylalanine replacement of tryptophan is expected to result in less structural perturbation (and thus in higher activity) than the alanine replacement, this observation seems counterintuitive. Among the W-to-A mutants, W400A (and, to a lesser extent, W377A) caused constitutive accumulation of higher levels of anthocyanin than the controls (Fig. 3 *A* and *B*), indicating again that W400A is constitutively active. All Trp-triad mutants of CRY1 were active in mediating blue light induction of mRNA expression of the three genes (*CHS, SIG5,* and *Psbs*) known to be induced by blue light (*SI Appendix,* Fig. S12). The constitutively active W400A mutant of CRY1 (and, to a lesser extent, W377A) exhibited constitutive activity stimulating mRNA expression of the *CHS* and *SIG5* genes but a light-dependent activity stimulating mRNA expression of the *Psbs* gene (*SI Appendix,* Fig. S12), suggesting that W400A may retain residual photo-responsiveness. In summary, all photoreduction-deficient Trp-triad mutants of CRY1 remained physiologically active in the three different blue light responses examined: inhibition of hypocotyl growth, promotion of anthocyanin accumulation, and change of gene expression. This result argues that the Trp triad-dependent rapid photoreduction is not required for the photophysiological activity of CRY1.

Trp Triad-Dependent Photoreduction Is Not Required for the Photobiochemical Activities of CRY1. A simple interpretation of the observation that all photoreduction-deficient CRY1 mutants retained physiological activities would be that the Trp-triad mutation did not disrupt the essential photochemical properties of CRY1 that are important to its functions. To test this proposition, we first examined the blue light-dependent phosphorylation of CRY1. *Arabidopsis* cryptochromes undergo blue light-dependent protein phosphorylation that is required for their photophysiological activities (35–39). Because phosphorylated CRY1 exhibits a blue light-dependent electrophoretic mobility upshift typical of phosphorylated proteins (36), we used the mobility upshift assay to test the blue light-dependent phosphorylation of the W-to-A Trp-triad mutants. As expected, the endogenous CRY1 and the wild-type GFP-CRY1 exhibited the blue light-dependent electrophoretic mobility upshift (Fig. 4 *A*

Fig. 3. The Trp-triad mutants of CRY1 are physiologically active in mediating blue light stimulation of anthocyanin accumulation. (*A* and *C*) Representative seedlings of the indicated genotypes are shown. Seedlings were grown on MS medium under continuous blue light (20 μmol·m⁻²·s⁻¹) or in darkness for 5 d. (*B* and *D*) Anthocyanin contents of seedlings of indicated genotypes. Seedlings were grown under the conditions in *A*. Anthocyanin was extracted from 30 seedlings per sample and is presented as (A530-A657)/ number of seedlings (*n* = 3). Error bars indicate SD.

and *B*). Similarly, the W324A and W377A Trp-triad mutants of CRY1, as well as mutations of the two non–Trp-triad tryptophan residues (W334A and W356A), also showed light-dependent mobility upshift (Fig. 4 *B–D*). The observation that both Trp-triad and non–Trp-triad mutants retained the photobiochemical activity is consistent with the results showing that both types of mutants retained the photophysiological activities (Fig. 3 and *SI Appendix,* Figs. S8 and S11). Importantly, the W400A mutant exhibited a constitutive mobility upshift that can be eliminated by the protein phosphatase treatment, demonstrating that W400A is constitutively phosphorylated independent of light (Fig. 4*C*). This result also is consistent with the fact that W400A is constitutively active in vivo (Fig. 3 and *SI Appendix,* Figs. S8 and S11).

Another known photobiochemical activity of CRY1 is its blue light-dependent physical interaction with SPA1 (SUPPRESSOR OF PHYTOCHROME A 1) (40, 41). Therefore, we tested whether the constitutively active Trp-triad mutation W400A may interact constitutively with SPA1. We first compared the activity of CRY1 and W400A, using the HEK 293 coexpression system and a coimmunoprecipitation assay. Fig. 4 shows that both the wild-type CRY1 protein and the W400A mutant protein coimmunoprecipitated SPA1 (Fig. 4 *E* and *F*). However, in
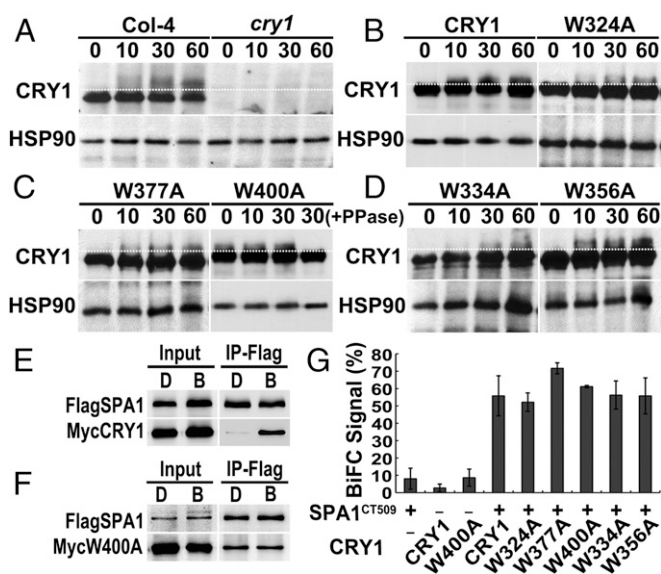
Fig. 4. The Trp-triad mutants of CRY1 are biochemically active. (A–D) Mobility upshift assay showing blue light-dependent phosphorylation of the endogenous CRY1 (Col-4), the GFP-CRY1 control (CRY1), and the indicated mutants of CRY1 and light-independent phosphorylation of the W400A mutant of CRY1. Seven-day-old seedlings grown on MS medium in darkness (0) were exposed to blue light (30 μmol·m^{-2}·s^{-1}) for 10, 30, or 60 min. Samples were extracted and fractionated in a 6% SDS/PAGE gel, blotted, probed with anti-CRY1 antibody, stripped, and reprobed with anti-HSP90 antibody. An aliquot of the W400A mutant from seedlings exposed to blue light for 30 min was treated with Lambda Protein Phosphatase [30(+PPase)]. White dotted lines are drawn to help distinguish the upshifted (i.e., phosphorylated) bands. Levels of proteins from different immunoblots are not directly comparable. (E and F) Coimmunoprecipitation assay showing the blue light-dependent CRY1–SPA1 interaction and the constitutive W400A–SPA1 interaction. CRY1 and SPA1 or W400A and SPA1 were coexpressed in HEK293 cells. The transfected cells were cultured in darkness before exposure to blue light (40 μmol·m^{-2}·s^{-1}) for 2 h or were kept in darkness. The total protein extracts (Input) and immunoprecipitation product (IP-Flag) were fractionated by a SDS/PAGE gel, blotted, probed with the anti-Flag antibody, stripped, and reprobed with the anti-CRY1 antibody. (G) Results of BiFC assays showing the interaction of the CRY1 or mutant proteins with SPA1^{CT509} in N. benthamiana plants. Three-week-old tobacco plants grown in long-day conditions (16 h light/8 h dark) were cotransformed with Agrobacteria harboring the plasmids encoding nYFP-CRY1^{W-to-A} mutants and cCFP-SPA1^{CT509}. The transformed plants were incubated for 12 h in the dark and then were transferred to white light for 48–72 h. The infected leaf spots were excised and examined under a fluorescence microscope. Images were taken at 10× magnification and are shown in SI Appendix, Fig. S14. The percentage of cells that exhibit BiFC fluorescence signals were calculated by the formula [(number of YFP fluorescent nuclei/number of DAPI-stained nuclei)%]. Data are shown as means and SD (n = 3).

contrast to the wild-type CRY1 recombinant protein that exhibited a blue light-dependent interaction with SPA1 (Fig. 4E), W400A showed constitutive interaction with SPA1 (Fig. 4F). This result is reminiscent of the W374A Trp-triad mutant of CRY2, which also exhibited constitutive physiological activities and constitutive interaction with SPA1 (22). We further tested whether the Trp-triad mutants of CRY1 may interact with SPA1 in plant cells. Because the CT509 fragment of SPA1 (SPA1^{CT509}), which contains the coiled-coil and WD domains known to interact constitutively with CRY1 and exert the physiological function of SPA1 (40, 41), is relatively easier to express, we tested whether the Trp-triad mutations of CRY1 can interact with SPA1^{CT509} in plant cells, using the bimolecular fluorescence complementation (BiFC) assay described previously (42). In this experiment, the Trp-triad mutants of CRY1 and SPA1^{CT509} were fused to the N-terminal fragment of YFP or to the C-terminal fragment of CFP, respectively; different

pairs of constructs were cotransfected to leaves of Nicotiana benthamiana; and the protein–protein interaction was analyzed semiquantitatively by measuring the percentage of cells that showed reconstituted YFP activity (Fig. 4G and SI Appendix, Figs. S13 and S14). Results of this experiment demonstrate that all Trp-triad mutants tested interacted with SPA1^{CT509} in plant cells (Fig. 4G and SI Appendix, Figs. S13 and S14). We concluded that the Trp-triad mutations of CRY1 retained the biochemical activities to undergo protein phosphorylation and protein–protein interaction, explaining why these photoreduction-deficient Trp-triad mutants of CRY1 are physiologically active in plants.

Discussion

We show in the present study that the Trp triad-dependent rapid photoreduction is not required for the photobiochemical and photophysiological activities of Arabidopsis CRY1 in plants. This result is consistent with similar findings in E. coli photolyase (16, 17), Drosophila cryptochrome (10, 13, 19–21), and Arabidopsis CRY2 (22). It has been proposed recently that ATP-enhanced photoreduction may rescue the defects of the Trp-triad mutants of Arabidopsis CRY2 in both photoreduction and physiological activities in plants (23). This hypothesis is attractive, because cryptochrome is known to bind ATP, and ATP may act as the phosphate donor for the light-dependent phosphorylation of cryptochromes (35–37). However, several observations are in contrast with what would be expected based on the ATP-enhanced photoreduction model. First, ATP enhances rapid photoreduction of wild-type CRY2 but not wild-type CRY1 (Fig. 1 C and F) (23). Second, ATP enhances light-dependent flavin reduction of the Trp-triad mutant W374A of CRY2 that is constitutively active in plants (22, 23), suggesting that the ATP-enhanced photoreduction is irrelevant to the light-independent physiological activities of the W374A mutant of CRY2. Third, ATP enhances photoreduction of two non–Trp-triad mutants of CRY1 (W334F and W356F) that show no defect in photoreduction or physiological activity. Finally, ATP does not enhance rapid photoreduction of the W397F mutant of CRY2 (23) or the W400F and W324A mutants of CRY1 (Fig. 1 D, E, G, and H), all of which possess light-dependent activities in plants (Figs. 2 and 3 and SI Appendix, Figs. S8–S12) (22). These observations demonstrate a lack of correlation between the ATP-enhanced photoreduction in vitro and the photophysiological activities of both CRY1 and CRY2 in vivo.

If the Trp-triad residues are not required for the photoexcitation of cryptochromes, why are they uniformly conserved in the photolyase/cryptochrome superfamily? To address this question, we analyzed the other two conserved tryptophan residues of CRY1 in this conserved region of the photolyase/cryptochrome proteins (Fig. 1B). We found that mutations of the evolutionarily conserved non–Trp-triad tryptophan residues of CRY1, W334 and W356, showed no apparent defects in photoreduction (Fig. 1 and SI Appendix, Fig. S1) or in the photophysiological or photobiochemical activities examined (Figs. 1–4 and SI Appendix, Figs. S8–S12). The observations that (i) the five tryptophan residues of this region are evolutionarily conserved regardless of a role in photoreduction and (ii) individual mutations of these conserved tryptophan residues failed to abolish CRY1 activities regardless of their respective photoreduction activity are consistent with the hypothesis that both the Trp-triad residues and the non–Trp-triad residues are evolutionarily conserved for reasons not directly associated with photoreduction per se. Taking together these results and those of previous studies, we argue that there is presently no genetic evidence to support the hypothesis that Trp triad-dependent photoreduction is the photoexcitation mechanism of cryptochromes. Renewed efforts are needed to elucidate the photoexcitation mechanism of the cryptochrome photoreceptors. For example, only rapid photoreduction (within 10 min) has been analyzed in this and previous studies, because the in vivo photobiochemical and photophysiological activities of plant cryptochromes

are detectable within ~10 min (35, 43). However, given that most photophysiological responses of plants endure prolonged light exposure for hours and days in nature, it would be interesting to examine how flavin photoreduction of cryptochromes under prolonged illumination may affect photophysiological activities of cryptochromes. Moreover, other types of electron movement, such as the circular electron shuttle mechanism of DNA photolyase (4, 14), may need to be explored to further understand the mechanism of cryptochrome photoexcitation.

Materials and Methods

Single amino acid substitutions of tryptophan to alanine or phenylalanine were introduced into the CRY1 coding region at the Trp-triad positions of 324, 377, and 400 and at the non–Trp-triad positions of 334 and 356, using the QuikChange Site-Directed Mutagenesis system according to the manufacturer's instruction (Stratagene). Transgenic lines expressing the recombinant GFP-CRY1 and GFP-CRY1 mutant proteins were prepared in the *cry1* mutant background (*cry1-304*, Col accession) (44). Additional methods of protein expression, purification, and analyses and the preparation and phenotypic analyses of transgenic plants are described in *SI Appendix*, *SI Materials and Methods*.

1. McCormick DB, Koster JF, Veeger C (1967) On the mechanisms of photochemical reductions of FAD and FAD-dependent flavoproteins. *Eur J Biochem* 2(4):387–391.
2. Penzer GR, Radda GK (1968) The chemistry of flavines and flavorproteins. Photoreduction of flavines by amino acids. *Biochem J* 109(2):259–268.
3. Cashmore AR (2003) Cryptochromes: Enabling plants and animals to determine circadian time. *Cell* 114(5):537–543.
4. Sancar A (2003) Structure and function of DNA photolyase and cryptochrome blue-light photoreceptors. *Chem Rev* 103(6):2203–2237.
5. Yu X, Liu H, Klejnot J, Lin C (2010) The cryptochrome blue-light receptors. *The Arabidopsis Book* (American Society of Plant Biologists, Rockville, MD), Vol 8, pp e0135, thearabidopsisbook.org, 10.1199/tab.0135.
6. Chaves I, et al. (2011) The cryptochromes: Blue light photoreceptors in plants and animals. *Annu Rev Plant Biol* 62:335–364.
7. Lin C, et al. (1995) Association of flavin adenine dinucleotide with the Arabidopsis blue light receptor CRY1. *Science* 269(5226):968–970.
8. Aubert C, Vos MH, Mathis P, Eker AP, Brettel K (2000) Intraprotein radical transfer during photoactivation of DNA photolyase. *Nature* 405(6786):586–590.
9. Hoang N, et al. (2008) Human and Drosophila cryptochromes are light activated by flavin photoreduction in living cells. *PLoS Biol* 6(7):e160.
10. Oztürk N, Song SH, Selby CP, Sancar A (2008) Animal type 1 cryptochromes. Analysis of the redox state of the flavin cofactor by site-directed mutagenesis. *J Biol Chem* 283(6):3256–3263.
11. Park HW, Kim ST, Sancar A, Deisenhofer J (1995) Crystal structure of DNA photolyase from *Escherichia coli*. *Science* 268(5219):1866–1872.
12. Giovani B, Byrdin M, Ahmad M, Brettel K (2003) Light-induced electron transfer in a cryptochrome blue-light photoreceptor. *Nat Struct Biol* 10(6):489–490.
13. Song SH, et al. (2007) Formation and function of flavin anion radical in cryptochrome 1 blue-light photoreceptor of monarch butterfly. *J Biol Chem* 282(24):17608–17612.
14. Liu B, Liu H, Zhong D, Lin C (2010) Searching for a photocycle of the cryptochrome photoreceptors. *Curr Opin Plant Biol* 13(5):578–586.
15. Zeugner A, et al. (2005) Light-induced electron transfer in Arabidopsis cryptochrome-1 correlates with its in vivo function. *J Biol Chem* 280(20):19437–19440.
16. Li YF, Sancar A (1990) Active site of *Escherichia coli* DNA photolyase: Mutations at Trp277 alter the selectivity of the enzyme without affecting the quantum yield of photorepair. *Biochemistry* 29(24):5698–5706.
17. Li YF, Heelis PF, Sancar A (1991) Active site of DNA photolyase: Tryptophan-306 is the intrinsic hydrogen atom donor essential for flavin radical photoreduction and DNA repair in vitro. *Biochemistry* 30(25):6322–6329.
18. Kavakli IH, Sancar A (2004) Analysis of the role of intraprotein electron transfer in photoreactivation by DNA photolyase in vivo. *Biochemistry* 43(48):15103–15110.
19. Gegear RJ, Foley LE, Casselman A, Reppert SM (2010) Animal cryptochromes mediate magnetoreception by an unconventional photochemical mechanism. *Nature* 463(7282):804–807.
20. Ozturk N, Selby CP, Annayev Y, Zhong D, Sancar A (2011) Reaction mechanism of Drosophila cryptochrome. *Proc Natl Acad Sci USA* 108(2):516–521.
21. Fedele G, et al. (2014) Genetic analysis of circadian responses to low frequency electromagnetic fields in Drosophila melanogaster. *PLoS Genet* 10(12):e1004804.
22. Li X, et al. (2011) Arabidopsis cryptochrome 2 (CRY2) functions by the photoactivation mechanism distinct from the tryptophan (trp) triad-dependent photoreduction. *Proc Natl Acad Sci USA* 108(51):20844–20849.
23. Engelhard C, et al. (2014) Cellular metabolites enhance the light sensitivity of Arabidopsis cryptochrome through alternate electron transfer pathways. *Plant Cell* 26(11):4519–4531.
24. Brautigam CA, et al. (2004) Structure of the photolyase-like domain of cryptochrome 1 from Arabidopsis thaliana. *Proc Natl Acad Sci USA* 101(33):12142–12147.
25. Frisell WR, Chung CW, MacKenzie CG (1959) Catalysis of oxidation of nitrogen compounds by flavin coenzymes in the presence of light. *J Biol Chem* 234(5):1297–1302.
26. Massey V, Palmer G (1966) On the existence of spectrally distinct classes of flavoprotein semiquinones. A new method for the quantitative production of flavoprotein semiquinones. *Biochemistry* 5(10):3181–3189.
27. Massey V, Stankovich M, Hemmerich P (1978) Light-mediated reduction of flavoproteins with flavins as catalysts. *Biochemistry* 17(1):1–8.
28. Müller P, et al. (2014) ATP binding turns plant cryptochrome into an efficient natural photoswitch. *Sci Rep* 4:5175.
29. Cailliez F, Müller P, Gallois M, de la Lande A (2014) ATP binding and aspartate protonation enhance photoinduced electron transfer in plant cryptochrome. *J Am Chem Soc* 136(37):12974–12986.
30. Ahmad M, Cashmore AR (1993) HY4 gene of *A. thaliana* encodes a protein with characteristics of a blue-light photoreceptor. *Nature* 366(6451):162–166.
31. Lin C, Ahmad M, Cashmore AR (1996) Arabidopsis cryptochrome 1 is a soluble protein mediating blue light-dependent regulation of plant growth and development. *Plant J* 10(5):893–902.
32. Onda Y, Yagi Y, Saito Y, Takenaka N, Toyoshima Y (2008) Light induction of Arabidopsis SIG1 and SIG5 transcripts in mature leaves: Differential roles of cryptochrome 1 and cryptochrome 2 and dual function of SIG5 in the recognition of plastid promoters. *Plant J* 55(6):968–978.
33. Fuglevand G, Jackson JA, Jenkins GI (1996) UV-B, UV-A, and blue light signal transduction pathways interact synergistically to regulate chalcone synthase gene expression in Arabidopsis. *Plant Cell* 8(12):2347–2357.
34. Wu G, Spalding EP (2007) Separate functions for nuclear and cytoplasmic cryptochrome 1 during photomorphogenesis of Arabidopsis seedlings. *Proc Natl Acad Sci USA* 104(47):18813–18818.
35. Shalitin D, et al. (2002) Regulation of Arabidopsis cryptochrome 2 by blue-light-dependent phosphorylation. *Nature* 417(6890):763–767.
36. Shalitin D, Yu X, Maymon M, Mockler T, Lin C (2003) Blue light-dependent in vivo and in vitro phosphorylation of Arabidopsis cryptochrome 1. *Plant Cell* 15(10):2421–2429.
37. Bouly JP, et al. (2003) Novel ATP-binding and autophosphorylation activity associated with Arabidopsis and human cryptochrome-1. *Eur J Biochem* 270(14):2921–2928.
38. Yu X, et al. (2007) Derepression of the NC80 motif is critical for the photoactivation of Arabidopsis cryptochrome CRY2. *Proc Natl Acad Sci USA* 104(17):7289–7294.
39. Tan S-T, Dai C, Liu H-T, Xue H-W (2013) Arabidopsis casein kinase1 proteins CK1.3 and CK1.4 phosphorylate cryptochrome2 to regulate blue light signaling. *Plant Cell* 25(7):2618–2632.
40. Lian HL, et al. (2011) Blue-light-dependent interaction of cryptochrome 1 with SPA1 defines a dynamic signaling mechanism. *Genes Dev* 25(10):1023–1028.
41. Liu B, Zuo Z, Liu H, Liu X, Lin C (2011) Arabidopsis cryptochrome 1 interacts with SPA1 to suppress COP1 activity in response to blue light. *Genes Dev* 25(10):1029–1034.
42. Meng Y, Li H, Wang Q, Liu B, Lin C (2013) Blue light-dependent interaction between cryptochrome2 and CIB1 regulates transcription and leaf senescence in soybean. *Plant Cell* 25(11):4405–4420.
43. Parks BM, Cho MH, Spalding EP (1998) Two genetically separable phases of growth inhibition induced by blue light in Arabidopsis seedlings. *Plant Physiol* 118(2):609–615.
44. Mockler TC, Guo H, Yang H, Duong H, Lin C (1999) Antagonistic actions of Arabidopsis cryptochromes and phytochrome B in the regulation of floral induction. *Development* 126(10):2073–2082.

Trp triad-dependent rapid photoreduction is not required for the function of Arabidopsis CRY1

Jie Gao[a,b,1], Xu Wang[b,c,1], Meng Zhang[d,e,1], Mingdi Bian[a,1], Weixian Deng[a], Zecheng Zuo[a], Zhenming Yang[a,2],Dongping Zhong[d,e,2], and Chentao Lin[b,2]

Supplemental Materials and Methods

Site-specific mutagenesis

Individual tryptophan residues of CRY1 at positions 324, 334, 356, 377, or 400 were substituted to alanine or phenylalanine using QuikChange Site-Directed Mutagenesis system according to the instruction manual (Stratagene).The sequences of primers used in site-directed mutagenesis are shown in the following:

W324A-F, CCATCTAAAGTTCTTCCCT**GCG**GCTGTGGATGAGAACTAT
W324A-R, ATAGTTCTCATCCACAGC**CGC**AGGGAAGAACTTTAGATGG
W377A-F, GTTAAAGTGCTTCAATTACCA**GCG**AGATGGGGGGATGAAGTATTTC
W377A-R, GAAATACTTCATCCCCCATCT**CGC**TGGTAATTGAAGCACTTTAAC
W400A-F, GAAAGCGATGCTCTTGGT**GCG**CAATACATTACCGGTAC
W400A-R, GTACCGGTAATGTATTG**CGC**ACCAAGAGCATCGCTTTC
W334A-F, TGAGAACTATTTCAAGGCA**GCG**AGGCAAGGCCGGACTGG
W334A-R, CCAGTCCGGCCTTGCCT**CGC**TGCCTTGAAATAGTTCTCA
W356A-F, GAGAGTTATGGGCTACTGGT**GCG**TTGCATGATCGCATAAGAG
W356A-R, CTCTTATGCGATCATGCAA**CGC**ACCAGTAGCCCATAACTCTC
W324F-F, CCATCTAAAGTTCTTCCCT**TTT**GCTGTGGATGAGAAC
W324F-R, GTTCTCATCCACAGC**AAA**AGGGAAGAACTTTAGATGG
W377F-F, GTGCTTCAATTACCA**TTT**AGATGGGGGGATGAAG
W377F-R, CTTCATCCCCCATCT**AAA**TGGTAATTGAAGCAC
W400F-F, GCGATGCTCTTGGT**TTT**CAATACATTACCGGTACTC
W400F-R, GAGTACCGGTAATGTATTG**AAA**ACCAAGAGCATCGC
W334F-F, GAGAACTATTTCAAGGCA**TTT**AGGCAAGGCCGGAC
W334F-R, GTCCGGCCTTGCCT**AAA**TGCCTTGAAATAGTTCTC
W356F-F, GGGCTACTGGT**TTT**TTGCATGATCGCATAAGAGTAG
W356F-R, CTACTCTTATGCGATCATGCAA**AAA**ACCAGTAGCCC

Expression, purification, and photoreduction assay

The mutated CRY1 cDNAs were cloned to the vector pFastBacHTA, by fusing CRY1 in frame to the C-terminus of His tag at the *Eco*RI and *Xho*I restriction sites of pFastBacHTA. The recombinant pFastBacHTA plasmids were transformed to DH10Bac™ *E. coli* to generate the recombinant Bacmids, which were used to transfect Sf9 insect cells using the Bac-to-Bac Baculovirus expression system according to the manufacturer's instruction (Invitrogen). The wild-type His-CRY1 protein and trp-triad mutant His-CRY1 proteins were purified using the Ni-NTA Purification System (Invitrogen) with minor modification. Briefly, the virus-infected

cells were centrifuged at 5,000 rpm for 5 min, suspended with Native Binding Buffer [500 mM NaCl, 50 mM NaH_2PO_4 (pH 8.0), 0.5% Triton X-100,1:3,000 β-mercaptoethanol, with 1 mM PMSF added freshly, pH 8.0]. The cells were lysed by sonication (model VC505; Sonics & Materials,Inc.) for 5 ×10 s at 30% amplitude until the solution became watery, and centrifuged at 14,000 rpm for 30 min at 4 °C. The supernatant was filtered with a 0.22-μm filter. Proteins were further purified according to the user manual of Ni-NTA Purification System (Invitrogen). For the photoreduction assays, the proteins were illuminated by blue light (450±15 nm, 1.8 mW·cm^{-2} or approximately 70 μmol·m^{-2}·s^{-1}) and absorption spectra were recorded at indicated times under anaerobic conditions at 20 °C, in the presence of 10 mM β-mercaptoethanol as external electron donor.

Plant materials

The mutated CRY1 cDNAs were cloned into the pEGAD vector, by fusing in frame to the C-terminus of GFP as described previously (1, 2). Transgenic lines expressing 35S::*GFP-CRY1*, 35S::*GFP-CRY1*$^{W-to-A}$ mutants, and 35S::*GFP-CRY1*$^{W-to-F}$ mutants were prepared in the *cry1-304* mutant background of the Col-0 accession (3). The *cry1* mutations of indicated transgenic lines were confirmed by genomic PCR, using primer pairs: CRY1^{N}F (5'-TTGCCA-GAGAGGCACTCAGAGAG) and CRY1^{N}R (5'- GGTGGAAGAAGAGGAGACTCAAGGG) spanning the sequence encoding the N-terminal fragment of *CRY1*.

Our repeated attempts to obtain the previously published transgenic lines expressing the W324F and W400F trp-triad mutants (4) were unsuccessful. Therefore, a direct comparison of the transgenic lines reported here and those reported previously (4) could not be performed.

Hypocotyl inhibition assay

Seedlings were prepared as described previously (2). Briefly, seeds were sterilized and sown on MS medium, stratified at 4 °C in darkness for 4 d, treated with white light for 24h to induce germination, transferred to the different light conditions for 5 d. Hypocotyl lengths were measured as described (5).

Anthocyanin extraction and quantization

Anthocyanin contents of transgenic lines expressing the CRY1^{W-to-A} mutants and CRY1^{W-to-F} mutants were measured as previously reported (6, 7). Seedlings were grown in continuous blue light (20 μmol·m^{-2}·s^{-1}) or darkness for 5 d. 30 seedlings per sample were frozen in liquid nitrogen, ground in liquid nitrogen in a 1.5 ml tube and total plant pigments were extracted overnight at room temperature in 0.8 ml methanol with 1% HCl. Samples were centrifuged in a microcentrifuge for 10 min, ca. 0.6 ml supernatant were moved to a new tube, and mixed with 0.4 ml H_2O and 0.6 ml chloroform. Samples were shaken for 1h, centrifuged to separate chlorophyll from anthocyanin, levels of anthocyanin in the methanol phase (upper) was determined spectrophotometrically and calculated by the formula (A530-A657)/ number of seedling ×1000 as described previously (8).

Phosphorylation and dephosphorylation assays

Seven-day-old etiolated transgenic seedlings grown on MS in darkness for were exposed to blue light (30 μmol·m^{-2}·s^{-1}) for the time indicated. For dephosphorylation assays, total protein was firstly extracted with protein extraction buffer [50 mM Tris-HCl pH 7.5, 150 mM NaCl, 1% Triton X-100], treated with Lambda Protein Phosphatase (NEB P0753S) in a reaction conditions [50 mM HEPES, 100 mM NaCl, 2 mM DTT, 0.01% Brij 35, 1mM $MnCl_2$] according to the user manual (NEB), incubated at 30°C for 30 min. The dephosphorylation

reaction was stopped by addition of the SDS/PAGE sample buffer and boiled for 2 min. Protein samples were fractionatedby a 6% (wt/vol) SDS/PAGE gel, blotted, probed with anti-CRY1 antibody, stripped and reprobed with HSP90 antibody as a loading control.

Protein expression in HEK293 (Human Embryonic Kidney) cells and co-immunoprecipitation assay

HEK293 (Human Embryonic Kidney) cell was cultured according to the Cell Culture Basics Handbook (invitrogen). Briefly, cells were maintained in Dulbecco's modified Eagle's medium (DMEM; Sigma) supplemented with 10% fetal calf serum and 1% penicillin/streptomycin (Gibco), cultured in 37°C incubator with a humidified atmosphere of 5% CO_2 in air. HEK293 cells were transfected by the calcium phosphate transfection method. Briefly, cells were plated the night before and grown to 60-70% confluence by the day of transfection. To transfect one well of cells in a 6-well plate, add < 2 μg DNA (for 6-well plates) to a 1.5 ml sterile tube, add ddH$_2$O to make the total volume of 180 μl, add 20 μl 2.5 M CaCl$_2$. When the DNA mixture is ready, add 200 μl of 2xHeBS [50 mM NaCl, 10 mM KCl, 1.5 mM Na$_2$HPO$_4$, 12 mM Dextrose(Mw: 180.16) and 50 mM Hepes(PH 7.5)] dropwise while vortex. Aspirate media from 6-well plates, slowly add the mixture to one side of the dish, and rotate to coat the whole well. Add 2 ml fresh media with 25 μM Chloriquine into the well, and incubate in 37°C incubator for 6 h to overnight. Aspirate the media with 25 μM Chloriquine, then change into 2 ml fresh media without Chioriquine. 30-48 h after transfection, the transfected cell cultured in darkness were exposed to blue light (40 μmol·m^{-2}·s^{-1}) or kept in darkness for 2 h. Cells were lysed in lysis buffer [1% Brij 35, 50 mM Tris pH=8.0, 150 mM NaCl, 1mM EDTA], and centrifuged to remove insoluble debris. The supernatants were pre-cleaned for 30 min with 20 ul protein G beads (PIERCE, Cat# 20398), mixed with EZview™ Red ANTI-FLAG® M2 Affinity Gel (SIGMA, Cat#F2426) and incubated for 1h. Beads were washed 5 times, spun briefly to remove supernatant. SDS/PAGE sample buffer was added into the immunoprecipitation products and boiled for 5 min. Total protein extracts (Input) and immunoprecipitation product (IP-Flag) were fractionated by a SDS/PAGE gel, transferred to nitrocellulose membranes, probed with the anti-Flag antibody, stripped, and reprobed with the anti-CRY1 antibody. In the co-IP assays, the plasmids encoding Myc-CRY1 /Myc-W400A, Flag-SPA1 and Myc-COP1 were co-expressed in HEK293 cells.

BiFC assay

The plasmids encoding nYFP-CRY1/CRY1^{W-to-A} mutants and cCFP-SPA1^{CT509} were constructed, transformed into Agrobacterium strain: Agl-0.The agrobacterium was cultured overnight in the LB medium [10 mM MES, 20 mM AS (Acetosyringone)] overnight, collected by centrifugation, washed and re-suspended in the infiltration buffer [10 mM MES, 150 mM AS, 10 mM MgCl2, 0.5% glucose]. Different Agrobacterial cultures were diluted to OD$_{600}$ = 0.5 and equal amounts of mixed, incubated at room temperature for 3 h, and infiltrated into three-week-old *Nicotiana benthamiana* leaves using a syringe as described before (9). The BiFC fluorescence signals were detected 2~3 d after infiltration by a Zeiss AxioImager Z1 microscope, images were taken by a Hamamatsu Orca-ER camera at 10×magnification or 100×magnification and processed by Zeiss Axiovision software.

mRNA expression assay

Total RNAs isolation, cDNA preparation and quantitative RT-PCR (qPCR) reactions were proceeded as described previously (2, 10). The qPCR signals of the *CHS* (At5g13930, chalcone synthase), *SIG5* (At5g24120, sigma factor 5), and *Psbs* (At1g44575, Chlorophyll a/b binding protein of photosystem II) genes were normalized to that of *ACT2* (At3g18780, actin 2) control. The primers used in the qPCR reaction of *CHS* and *ACT2* genes were as described (2). Primers used in the qPCR reaction of other genes are:

3

AtSIG5F (5'- TGATATAGTGAGCTTGGACTGG),
AtSIG5R (5'-CTTGCAGCTCTACCTATTTCG);
PsbsF (5'- CTCTTCAAACCCAAAACCAAAGCT),
PsbsR (5'- GCCTTTGTGAAACCAATCCCA).

References:

1. Yu, X., Sayegh, R., Maymon, M., Warpeha, K., Klejnot, J., Yang, H., Huang, J., Lee, J., Kaufman, L. & Lin, C. (2009) Formation of nuclear bodies of Arabidopsis CRY2 in response to blue light is associated with its blue light-dependent degradation. Plant Cell 21: 118-30.
2. Li, X., Wang, Q., Yu, X., Liu, H., Yang, H., Zhao, C., Liu, X., Tan, C., Klejnot, J., Zhong, D. & Lin, C. (2011) Arabidopsis cryptochrome 2 (CRY2) functions by the photoactivation mechanism distinct from the tryptophan (trp) triad-dependent photoreduction. Proc Natl Acad Sci U S A 108: 20844-9.
3. Mockler, T. C., Guo, H., Yang, H., Duong, H. & Lin, C. (1999) Antagonistic actions of Arabidopsis cryptochromes and phytochrome B in the regulation of floral induction. Development 126: 2073-82.
4. Zeugner, A., Byrdin, M., Bouly, J. P., Bakrim, N., Giovani, B., Brettel, K. & Ahmad, M. (2005) Light-induced electron transfer in Arabidopsis cryptochrome-1 correlates with in vivo function. J Biol Chem 280: 19437-40.
5. Yu, X., Klejnot, J., Zhao, X., Shalitin, D., Maymon, M., Yang, H., Lee, J., Liu, X., Lopez, J. & Lin, C. (2007) Arabidopsis cryptochrome 2 completes its posttranslational life cycle in the nucleus. Plant Cell 19: 3146-3156.
6. Chory, J. (1992) A genetic model for light-regulated seedling Arabidopsis. Development 115: 337-354.
7. Rabino, I. & Mancinelli, A. L. (1986) Light, Temperature, and Anthocyanin Production. Plant Physiology 81: 922-924.
8. Kubasek, W. L., Shirley, B. W., McKillop, A., Goodman, H. M., Briggs, W. & Ausubel, F. M. (1992) Regulation of Flavonoid Biosynthetic Genes in Germinating Arabidopsis Seedlings. The Plant Cell 4: 1229-1236.
9. Meng, Y., Li, H., Wang, Q., Liu, B. & Lin, C. (2013) Blue Light‚ÄìDependent Interaction between Cryptochrome2 and CIB1 Regulates Transcription and Leaf Senescence in Soybean. The Plant Cell Online 25: 4405-4420.
10. Liu, H., Yu, X., Li, K., Klejnot, J., Yang, H., Lisiero, D. & Lin, C. (2008) Photoexcited CRY2 interacts with CIB1 to regulate transcription and floral initiation in Arabidopsis. Science 322: 1535-9.

Supplemental Table

Table S1

CRY1 Proteins	Mutation	Trp-triad	Photoreduction	ATP-enhanced Photoreduction	Relative Expression	Photophysiological Activities			Photobiochemical Activities	
						Hypcotyl inhibition	Anthocyanin accumulation	Gene expression	B-induced phosphorylation	CRY1-SPA1^{CT509} interaction
WT	no	-	n/a	n/a	0.3	+	+	+	+	n/a
cry1	null	-	n/a	n/a	0	-	-	-	-	n/a
CRY1	no	-	+	-	1	++	++	++	++	++
CRY1^{W324A}	W324A	+	-	-	0.7	++	++	++	++	++
CRY1^{W324F}	W324F	+	-	+	0.6	++	++	n/a	n/a	n/a
CRY1^{W377A}	W377A	+	-	+	0.4	+++	++	++	++	++
CRY1^{W377F}	W377F	+	-	+	0.5	++	++	n/a	n/a	n/a
CRY1^{W400A}	W400A	+	n/a	n/a	0.7	+++	+++	+++	+++	++
CRY1^{W400F}	W400F	+	-	-	0.9	++	++	n/a	n/a	n/a
CRY1^{W334A}	W334A	-	n/a	n/a	0.8	++	++	++	++	++
CRY1^{W334F}	W334F	-	+	+	0.9	++	++	n/a	n/a	n/a
CRY1^{W356A}	W356A	-	+	n/a	1.1	++	++	++	++	++
CRY1^{W356F}	W356F	-	+	+	0.7	++	++	n/a	n/a	n/a

Table S1. The level of protein expression and activities of the trp-triad mutants of CRY1 in Arabidopsis plants.

The level of protein expression and light-responsive biochemical or physiological activities of the endogenous CRY1 (WT), the wild-type GFP-CRY1 control (CRY1) and the indicated mutants of CRY1 expressed in the *cry1* mutant parent are shown. The symbols "+" indicates light-dependent activity comparable to that of the endogenous CRY1 of the wild-type plants (WT), "++" indicates light-dependent activity comparable to the GFP-CRY1 control (CRY1), "+++" indicates constitutive activity, "na" indicates not analyzed.

Supplemental Figures
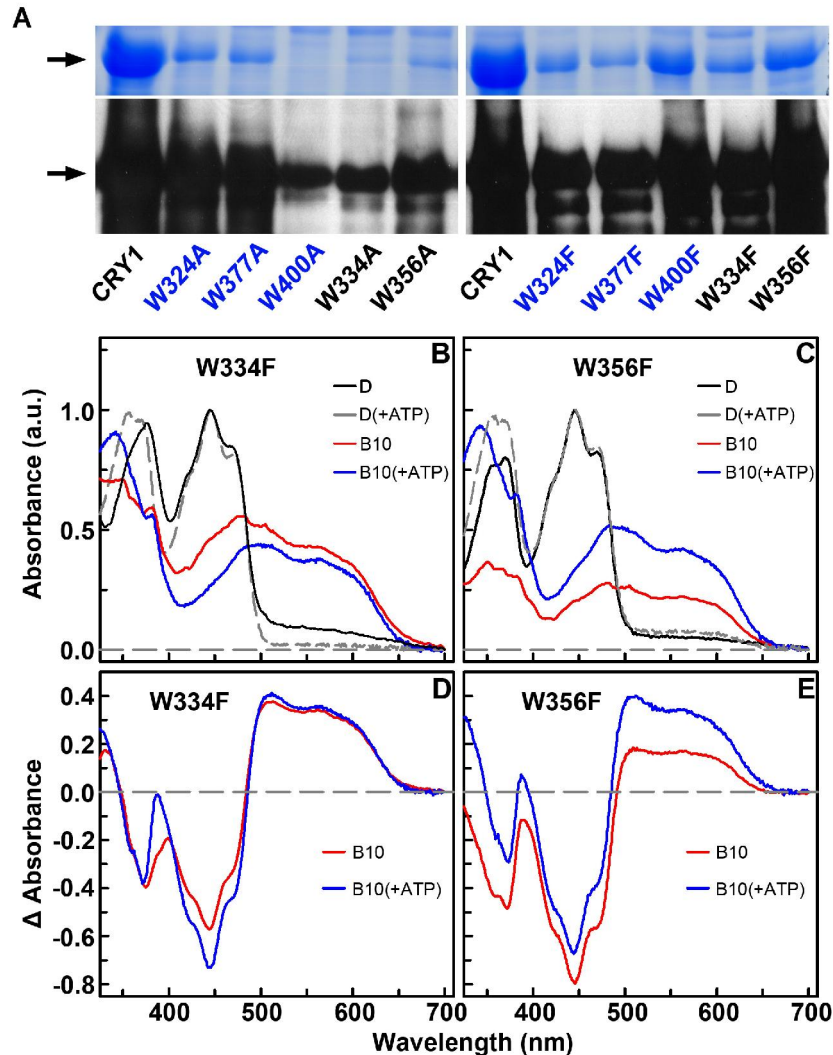
Fig. S1 Expression and purification of the CRY1 and indicated mutant proteins and photoreduction of the non-trp-triad W334F and W356F mutant proteins.
(A) Wild-type CRY1 and the CRY1 mutant proteins were expressed and purified from insect cells (Sf9), fractionated in 10% SDS/PAGE gel, stained with Coomassie Brilliant Blue (upper) or proceed with an immunoblot (lower), probed with anti-CRY1 antibody. Expression Levels of proteins from different gels or immunoblots are not directly comparable.
(B-C) The scanning absorption spectra of the non-trp-triad mutants W334F and W356F were recorded after blue light (450±15 nm, 1.8 mW·cm^{-2} or 70 μmol m^{-2}s^{-1}) treatment for 10 min in the absence (B10) or presence of 1mM ATP [B10 (+ATP)] under anaerobic conditions at 20 °C, in the presence of 10 mM β-mercaptoethanol as external electron donor. The absorption spectra of W334F in darkness are included, because the W334F protein tends to aggregate during experiment in darkness in the presence of ATP, reducing absorption and causing distorted differential spectrum shown in D.
(D-E) The difference spectra of W334F (D) and W356F (E) in the absence (B10) or presence of ATP [B10(+ATP]. The ATP enhancement of photoreduction of W334F was slightly underestimated due to protein aggregation of W334F in darkness in the presence of ATP (see B).

Fig. S2
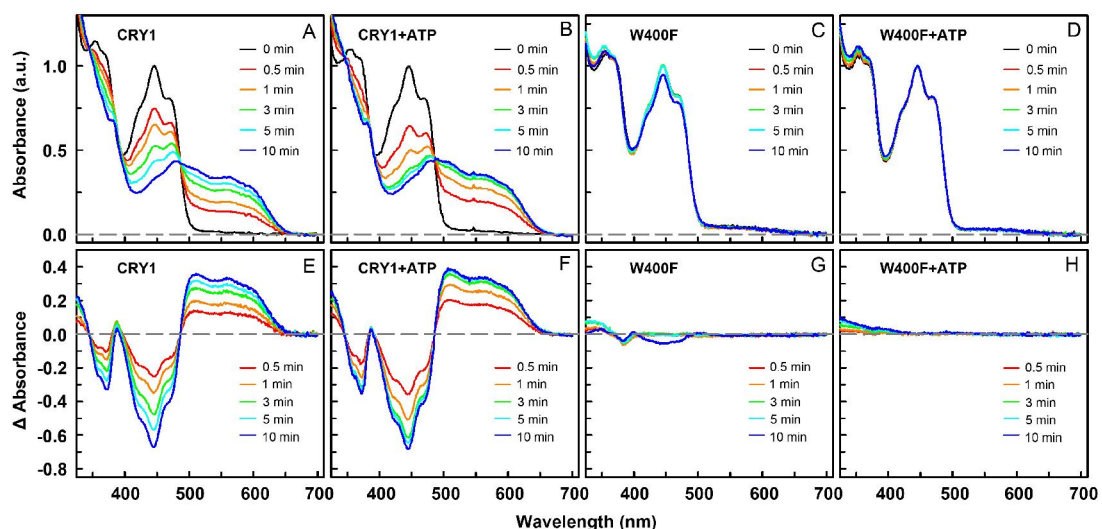
Fig. S2 Photoreduction of the wild-type CRY1 protein and the trp-triad W400F mutant protein.
(A-B) The scanning absorption spectra of the wild-type CRY1 protein purified from insect cells were recorded after blue light (450±15 nm, 1.8 mW·cm^{-2} or 70 µmol m^{-2}s^{-1}) treatment for the time indicated in the absence (A) or presence of 1mM ATP (B) under anaerobic conditions at 20 °C, in the presence of 10 mM β-mercaptoethanol as external electron donor.
(C-D) The scanning absorption spectra of the mutant W400F protein purified from insect cells were recorded after blue light (450±15 nm, 1.8 mW·cm^{-2} or 70 µmol m^{-2}s^{-1}) treatment for the time indicated in the absence (C) or presence of 1mM ATP (D) under anaerobic conditions at 20 °C, in the presence of 10 mM β-mercaptoethanol as external electron donor.
(E-F) The difference spectra of the wild-type CRY1 proteins in the absence (E) or presence (F) of ATP.
(G-H) The difference spectra of W400F in the absence (G) or presence (H) of ATP.
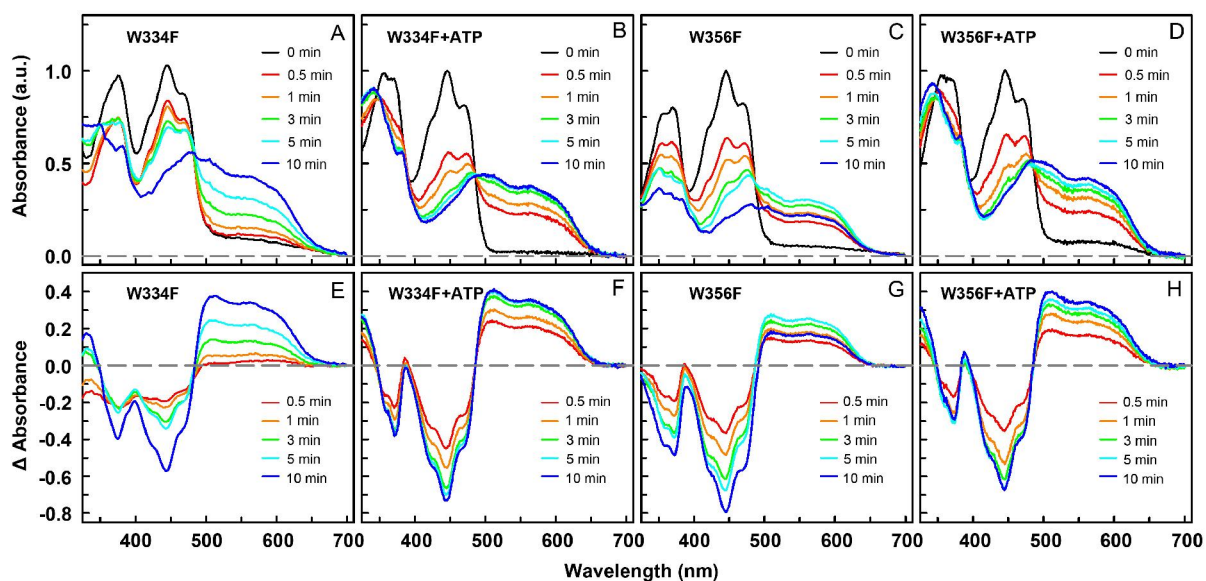
Fig. S3
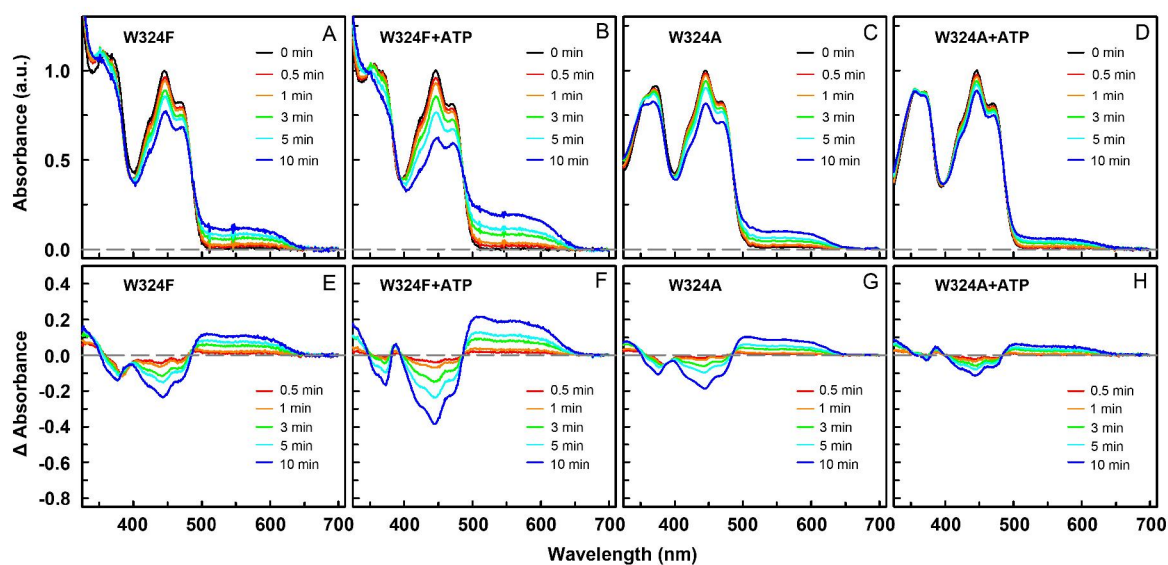
Fig. S3 Photoreduction of the trp-triad W324F and W324A mutant proteins.
(A-D) The scanning absorption spectra of the W324F (A-B) and W324A (C-D) mutant proteins purified from insect cells were recorded after blue light (450±15 nm, 1.8 mW·cm^{-2} or 70 μmol m^{-2}s^{-1}) treatment for the time indicated in the absence (A, C) or presence of 1mM ATP (B, D) under anaerobic conditions at 20 °C, in the presence of 10 mM β-mercaptoethanol as external electron donor.
(E-H) The difference spectra of the W324F (E-F) and W324A (G-H) mutant proteins in the absence (E, G) or presence (F, H) of ATP.

Fig. S4
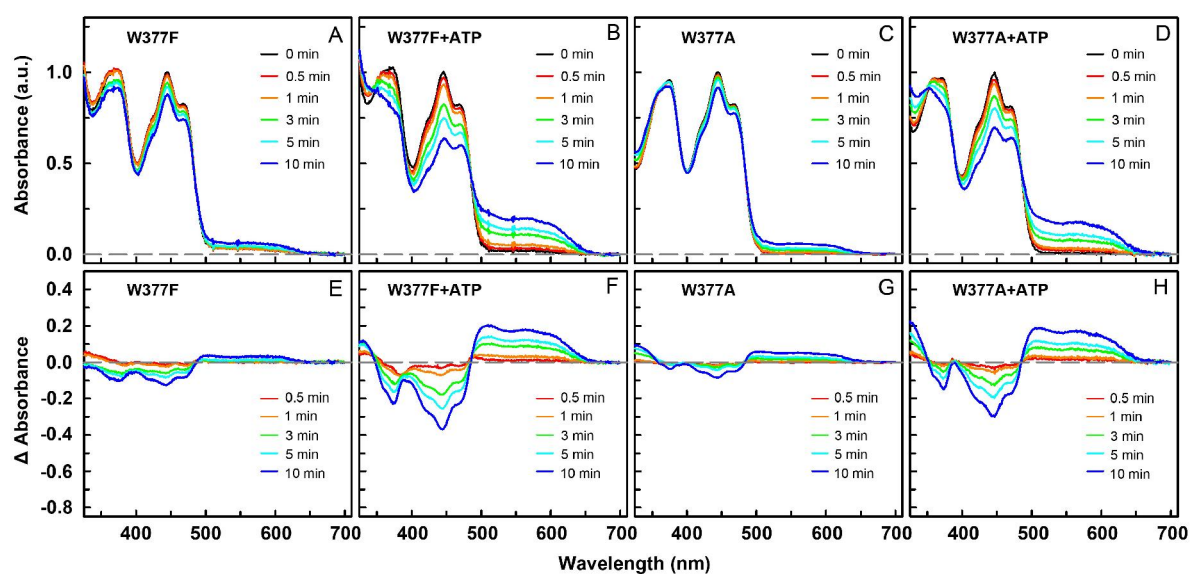
Fig. S4 Photoreduction of the trp-triad W377F and W377A mutant proteins.
(A-D) The scanning absorption spectra of the W377F (A-B) and W377A (C-D) mutant proteins purified from insect cells were recorded after blue light (450±15 nm, 1.8 mW·cm^{-2} or 70 µmol m^{-2}s^{-1}) treatment for the time indicated in the absence (A, C) or presence of 1mM ATP (B, D) under anaerobic conditions at 20 °C, in the presence of 10 mM β-mercaptoethanol as external electron donor.
**(E-H)** The difference spectra of the W377F (E-F) and W377A (G-H) mutant proteins in the absence (E, G) or presence (F, H) of ATP.

9

Fig. S5

Fig. S5 Photoreduction of the non-trp-triad W334F and W356F mutant proteins.
(A-D) The scanning absorption spectra of the W334F (A-B) and W356F (C-D) mutant proteins purified from insect cells were recorded after blue light (450±15 nm, 1.8 mW·cm^{-2} or 70 µmol m^{-2}s^{-1}) treatment for the time indicated in the absence (A, C) or presence of 1mM ATP (B, D) under anaerobic conditions at 20 °C, in the presence of 10 mM β-mercaptoethanol as external electron donor.
(E-H) The difference spectra of the W334F (E-F) and W356F (G-H) mutant proteins in the absence (E, G) or presence (F, H) of ATP.

10
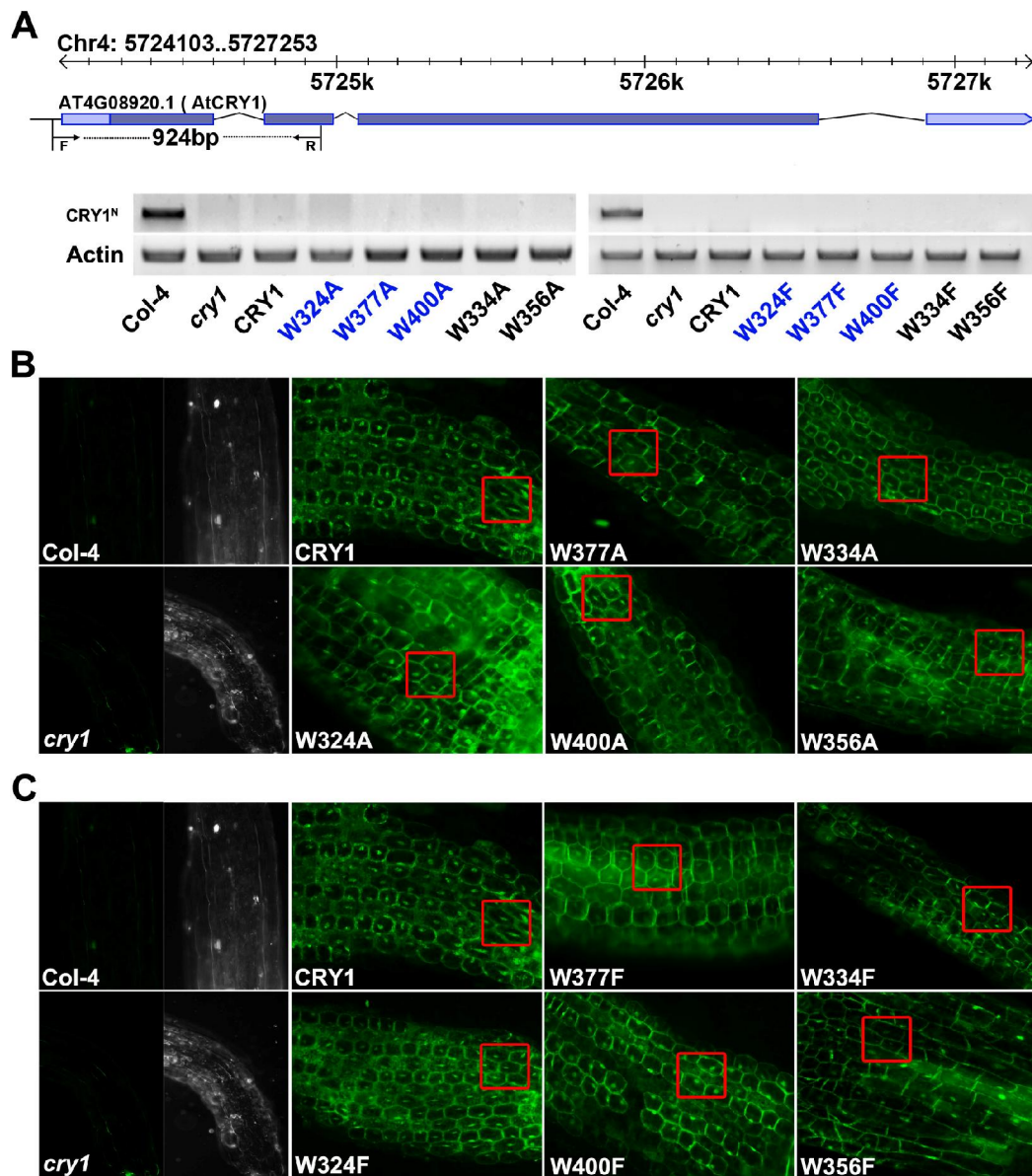
Fig. S6 Characterization of the GFP-CRY1 control and the trp-triad GFP-CRY1 mutant proteins.
(A) Verification of the *cry1* mutant background of the indicated transgenic lines. A diagram showing the *CRY1* locus and the positions of primer pairs used in the PCR reactions (Top), and DNA gels showing the genomic PCR product amplified from the genomic DNA isolated from the indicated genotypes (Bottom) are shown. The genomic DNAs were extracted using CTAB method from the 3-week-old respective transgenic lines grown in 16h light/8h darkness condition.
(B-C) Subcellular localization of the GFP-CRY1 and GFP-CRY1 mutants. 5~7-day-old seedlings were grown on MS medium under continuous white light, epidermis of hypocotyl was peeled for fluorescence microscopy analyses. Images were taken using a Zeiss AxioImager Z1 microscope, by a Hamamatsu Orca-ER camera at 10×Magnification, and processed by the Zeiss Axiovision software. Enlarged partial images (red square) are shown in Fig.S7.

Fig. S7
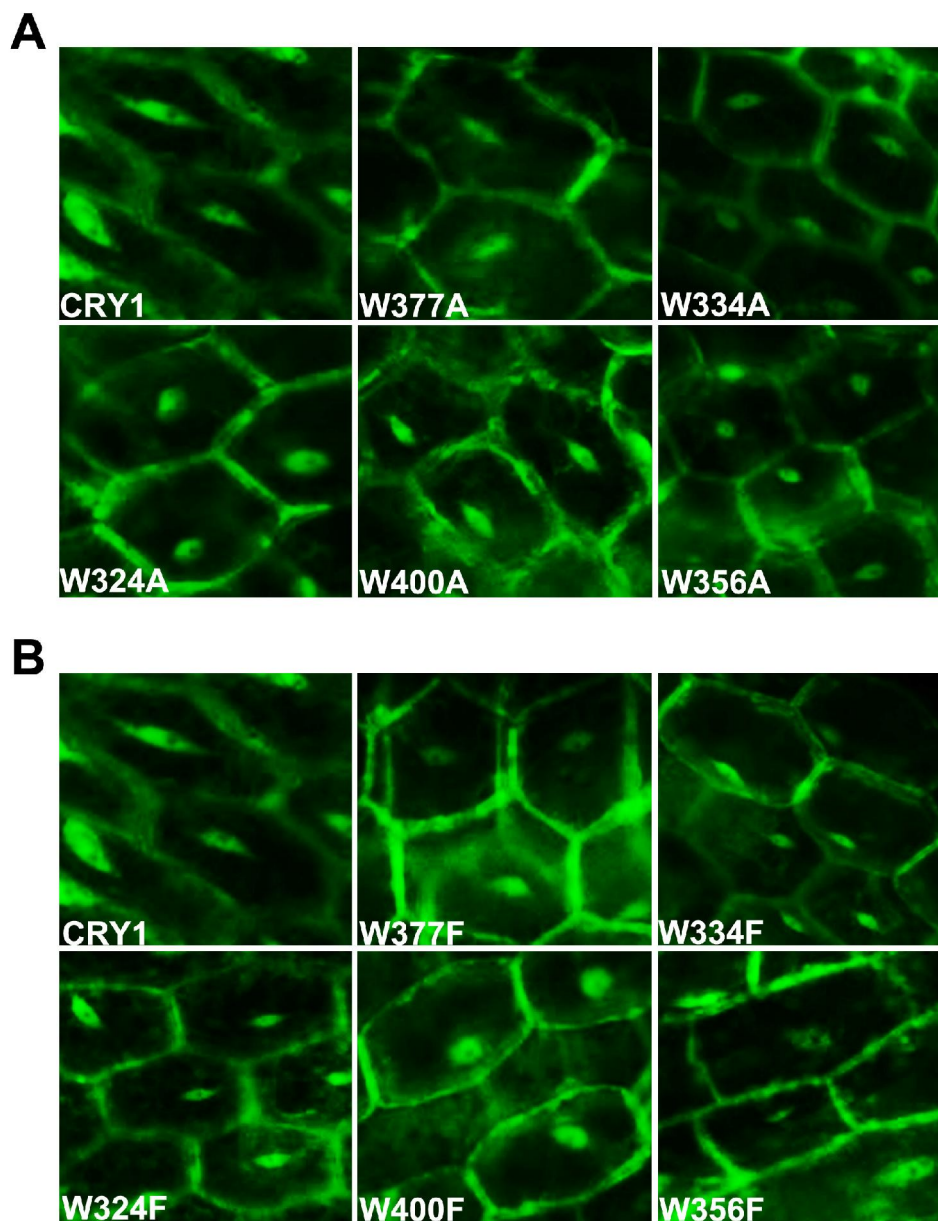
Fig.S7. The GFP-fusion proteins of the trp-triad mutants of CRY1 and the wild-type GFP-CRY1 controls are located in both the nucleus and cytosol. Seedlings grown condition and images capture were processed as described in Fig. S6. The amplified images of GFP-CRY1^{W-to-A} and GFP-CRY1^{W-to-F} trp-triad mutants in Fig.S6 are shown in (A) and (B), respectively.

Fig. S8
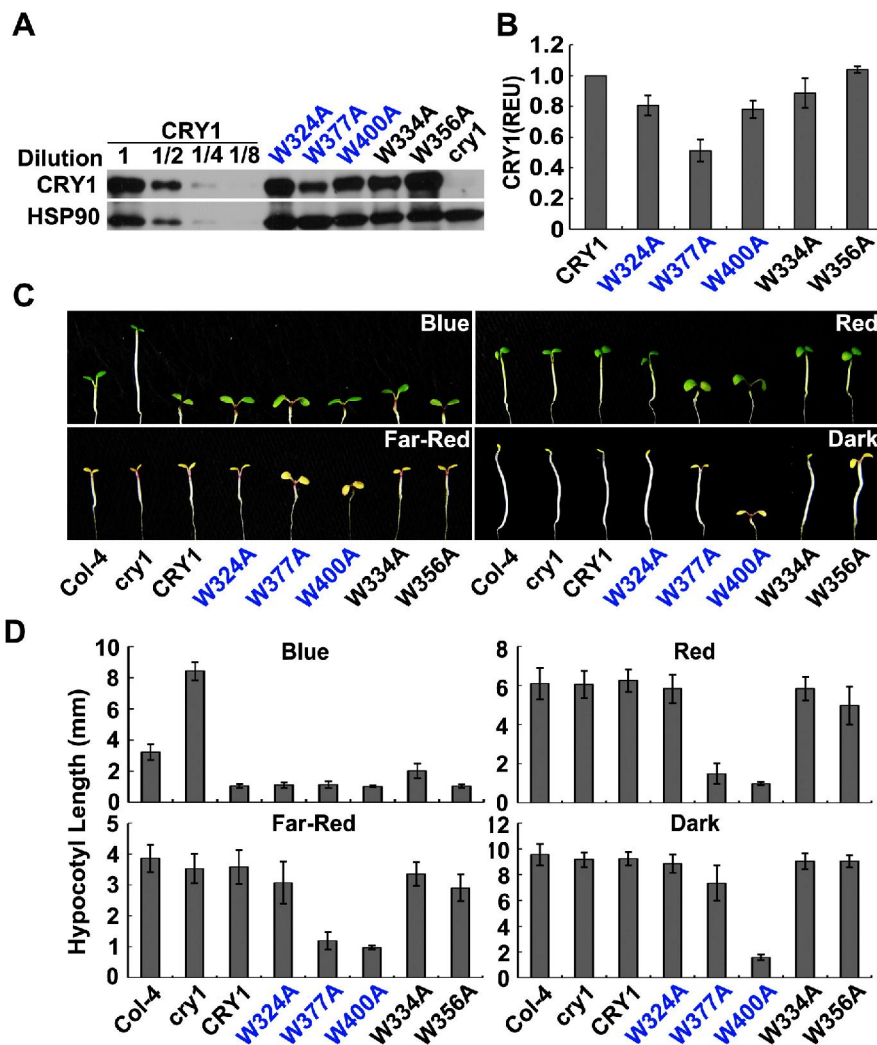
Fig. S8. The trp-triad mutants (W-to-A) of CRY1 are active in mediating blue light inhibition of hypocotyl elongation.
(A) Immunoblot showing the expression levels of GFP-fusion proteins of the trp-triad (labled in blue) and non-trp-triad mutants of CRY1 in transgenic plants. All transgenic lines are in the *cry1* background. Samples were extracted from seedlings grown on MS medium under continuous white light, fractionated in SDS/PAGE (10%), blotted, probed with anti-CRY1 antibody (CRY1), stripped, and reprobed with anti-HSP90 antibody (HSP90; Santa Cruz Biotechnology) as the loading control. A series dilution of the sample prepared from plants expressing the GFP-CRY1 control (CRY1), and the parental *cry1* mutant (*cry1*) are included to facilitate semi-quantification.
(B) The relative expression unit (REU) showing the semi-quantification of the indicated proteins was calculated by the formula $[CRY1^{mt}/HSP90^{mt}]/[CRY1^{wt}/HSP90^{wt}]$. The "CRY1" and "HSP90" signals of immunoblots were digitized and quantified by ImageJ.
(C) Images showing the representative seedlings of indicated genotypes. Seedlings were grown on MS medium under continuous blue light (20 $\mu mol \cdot m^{-2} \cdot s^{-1}$), red light (18 $\mu mol \cdot m^{-2} \cdot s^{-1}$), far-red light (1.5 $\mu mol \cdot m^{-2} \cdot s^{-1}$), or in darkness for 5 d.
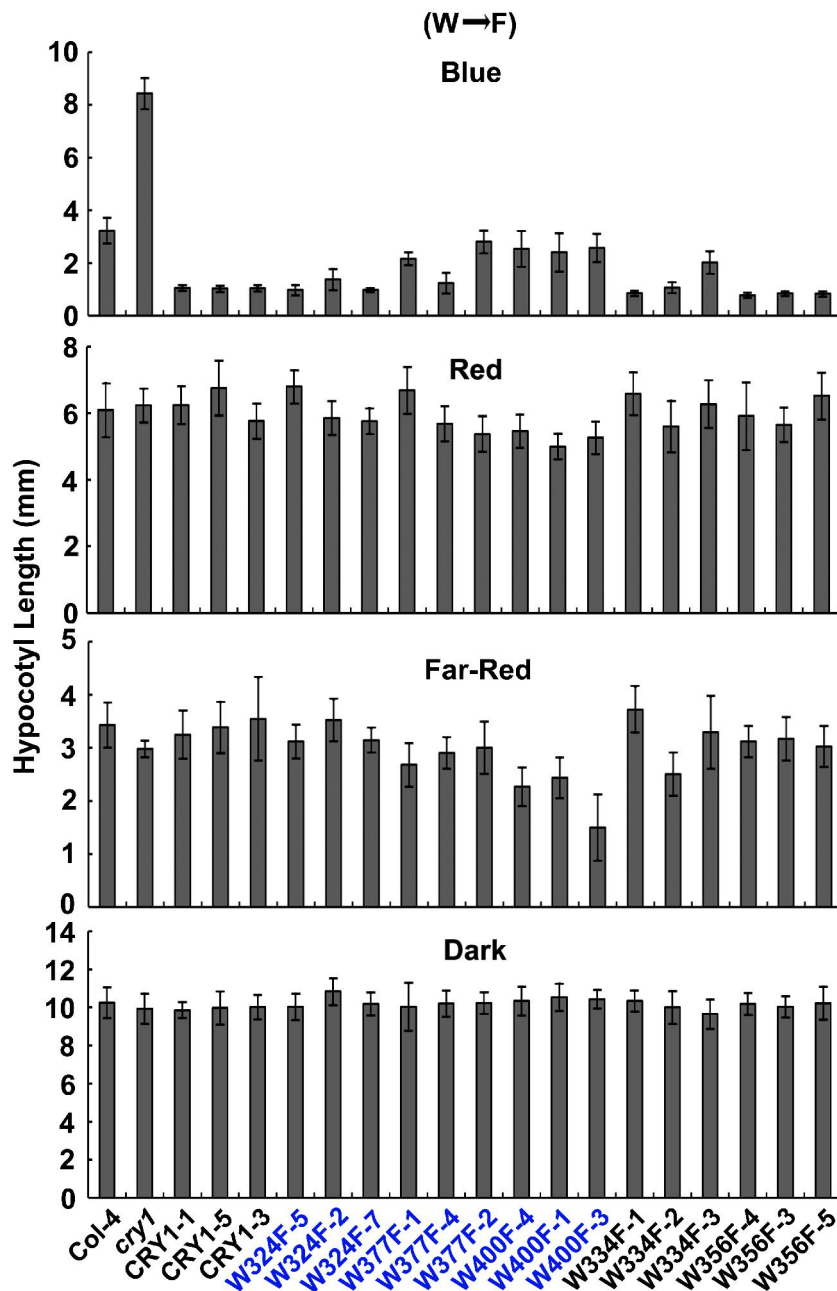**(D)** Hypocotyl lengths of indicated genotypes grown under conditions indicated in C were measured (n≥20). The wild-type plants (Col-4), the *cry1* mutant parent (*cry1*), and transgenic plants expressing the wild-type GFP-CRY1 (CRY1) controls are included. Error bars indicate SD.

13
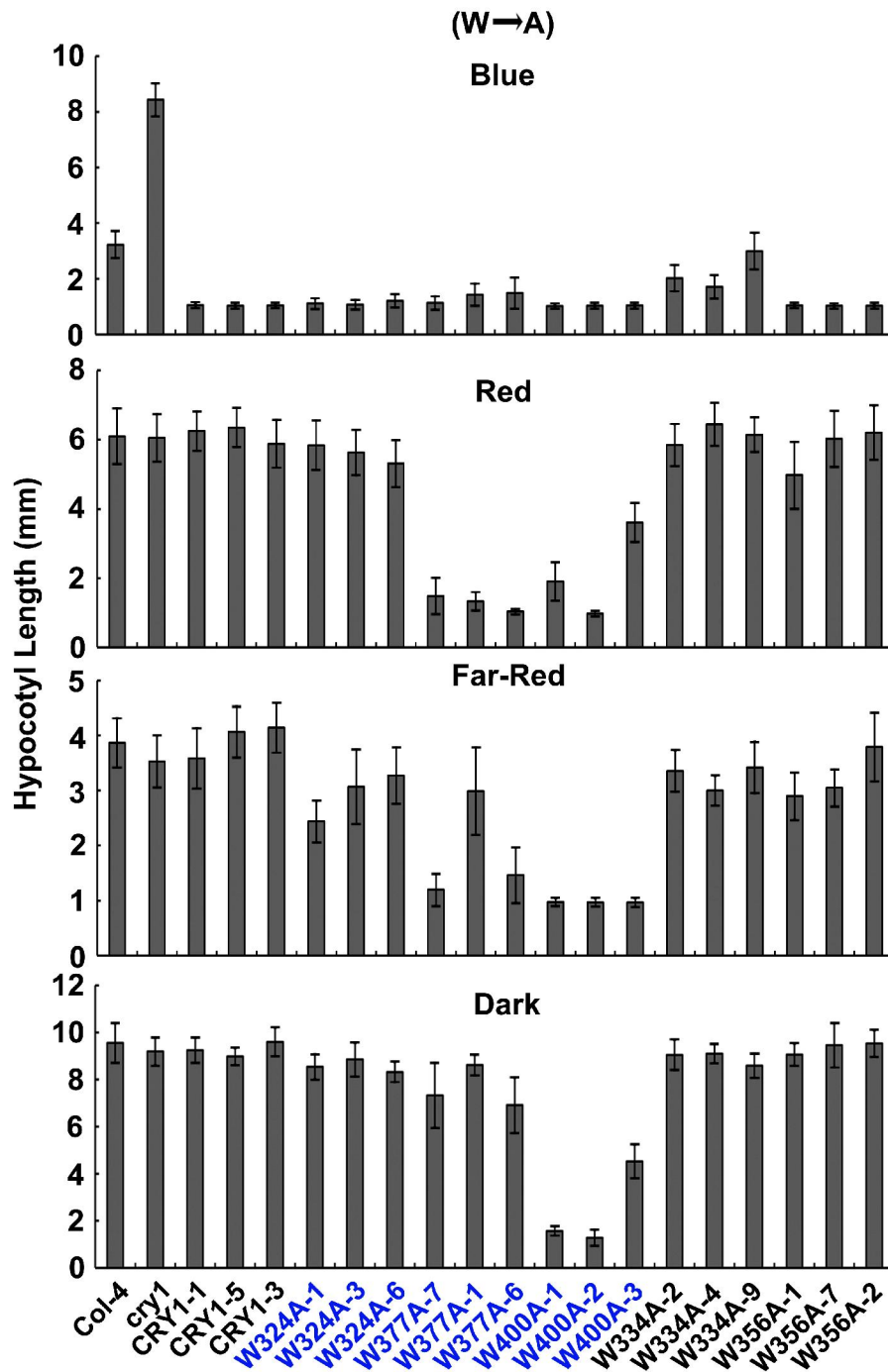
Fig. S9

Fig.S9. Hypocotyl inhibition phenotype of independent transgenic lines expressing wild-type GFP-CRY1 or the W-to-A mutants. Seedlings were grown under different light conditions as indicated, and hypocotyl lengths of indicated genotypes in independent transgenic lines were measured and shown with SD (n≥20). The trp-triad transgenic lines are highlighted in blue.
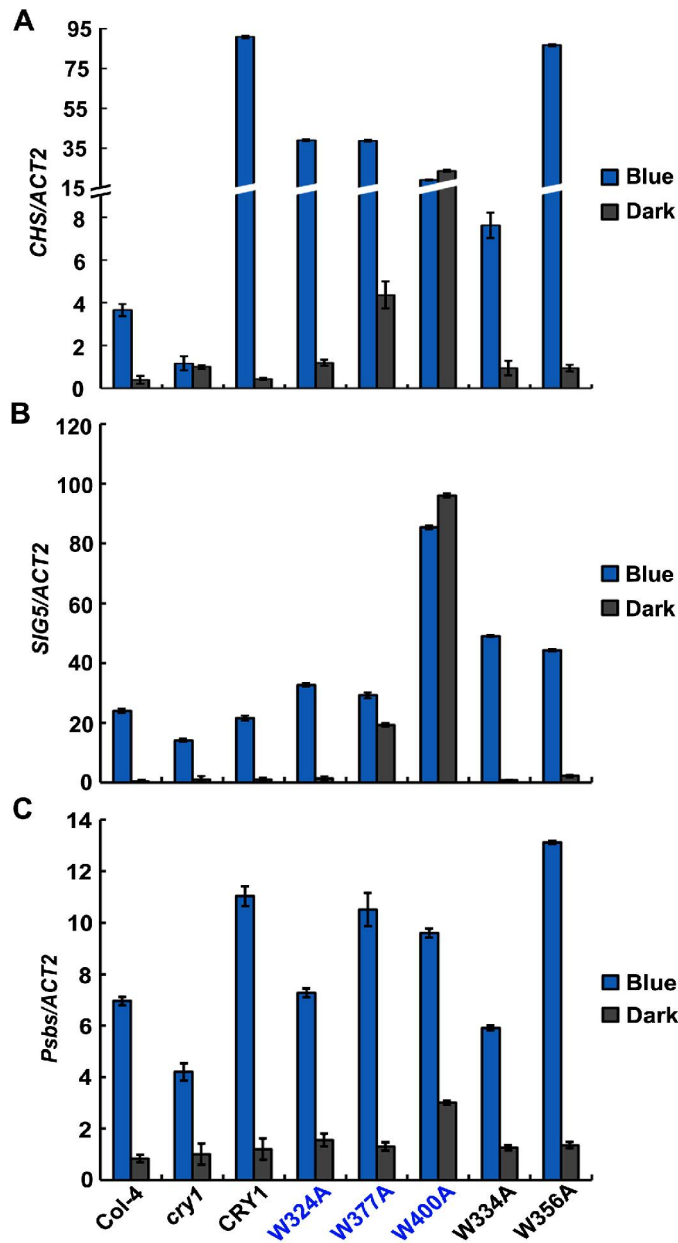
Fig. S10

Fig.S10. Hypocotyl inhibition phenotype of independent transgenic lines expressing wild-type GFP-CRY1 or the W-to-F mutants. Seedlings were grown under different light conditions as indicated, and hypocotyl lengths of indicated genotypes in independent transgenic lines were measured and shown with SD (n≥20). The trp-triad transgenic lines are highlighted in blue.

Fig. S11
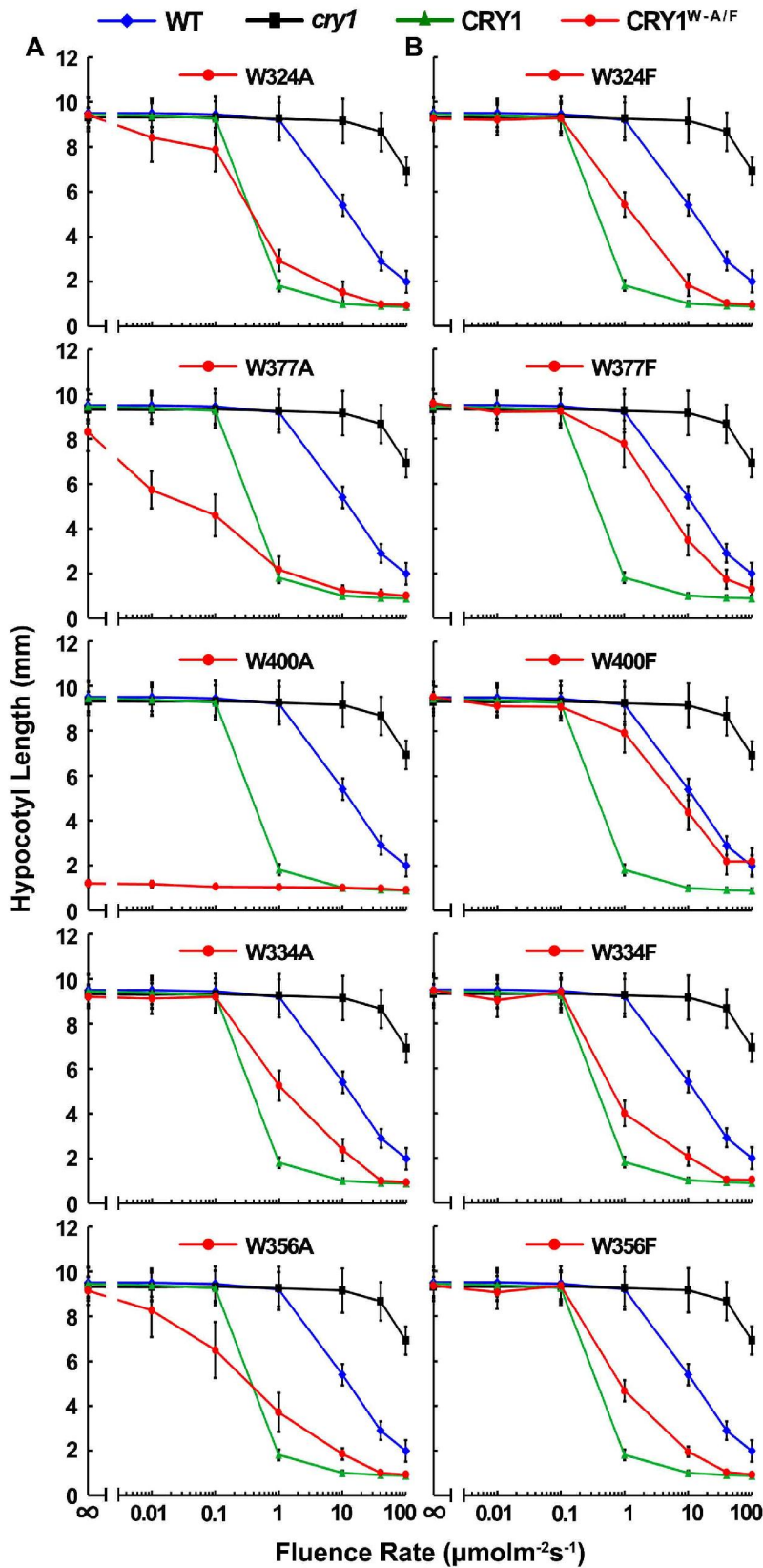
Fig. S11. The fluence-rate response analysis of the hypocotyl inhibition activities of CRY1 and the indicated mutants of CRY1.

5-day-old seedlings were grown on MS medium under continuous blue light of different fluence rates or in darkness. Hypocotyl lengths of indicated genotypes were measured and shown with SD (n≥20). The fluence rates are shown in the logarithmic scale, and the darkness is indicated by ∞.

16

Fig. S12

Fig.S12. Blue light-induced gene expression of transgenic lines expressing the indicated CRY1 mutants.
qPCR analysis of the mRNA expression of chalcone synthase (A, *CHS*), Sigma Factor 5 (B, *SIG5*) and photosystem II subunits (C, *Psbs*) genes in plants expressing the GFP-CRY1 or GFP-CRY1$^{\text{W-to-A}}$ trp-triad mutants. Total RNA was extracted from 7-d-old seedlings grown in darkness or continuous blue light (20 µmol·m^{-2}·s^{-1}). The qPCR signals of the respective genes are normalized to that of *ACT2* and shown with SD (n=3).
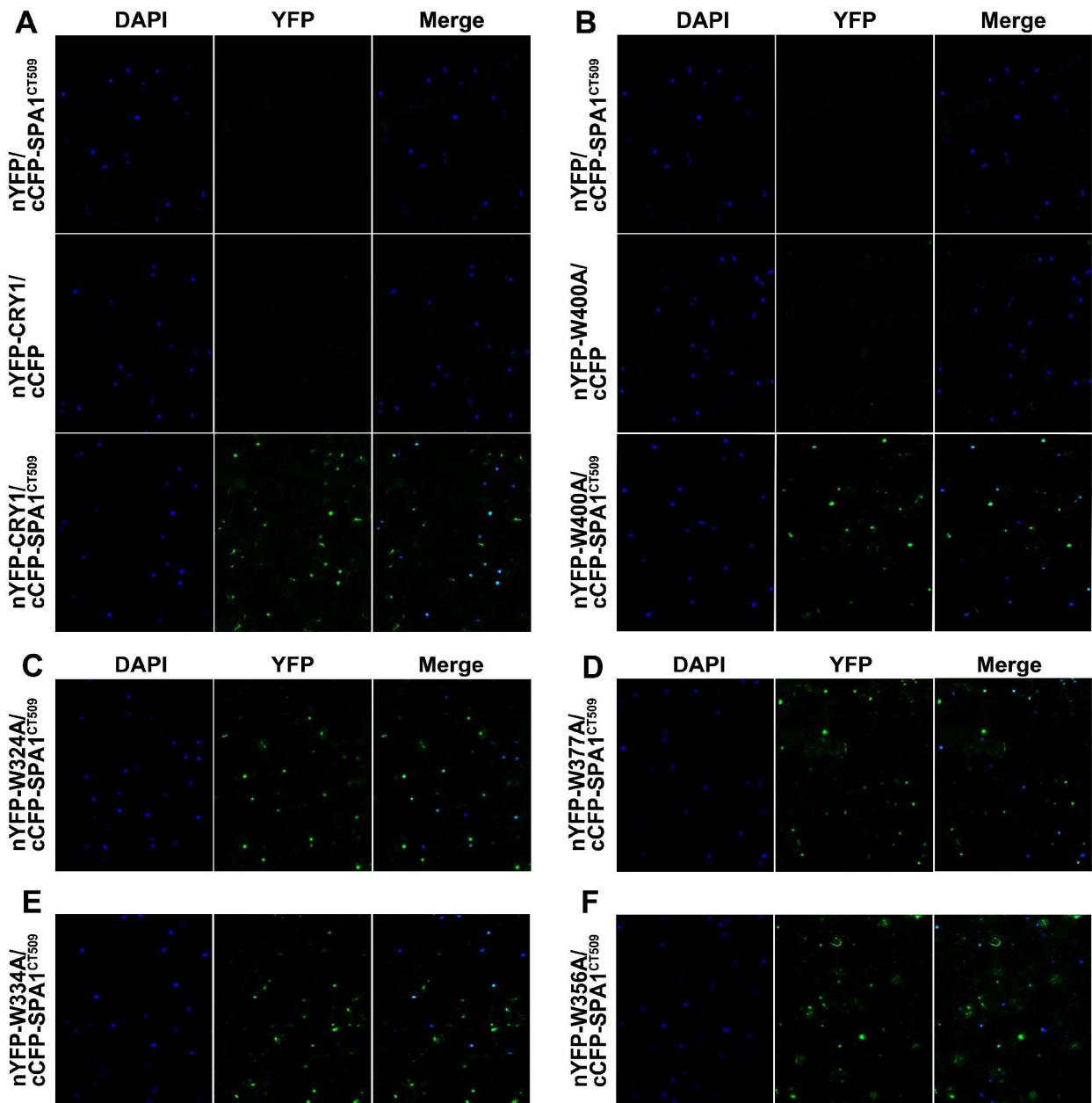
| | Cy3+DAPI | Cy3+YFP | Merge |
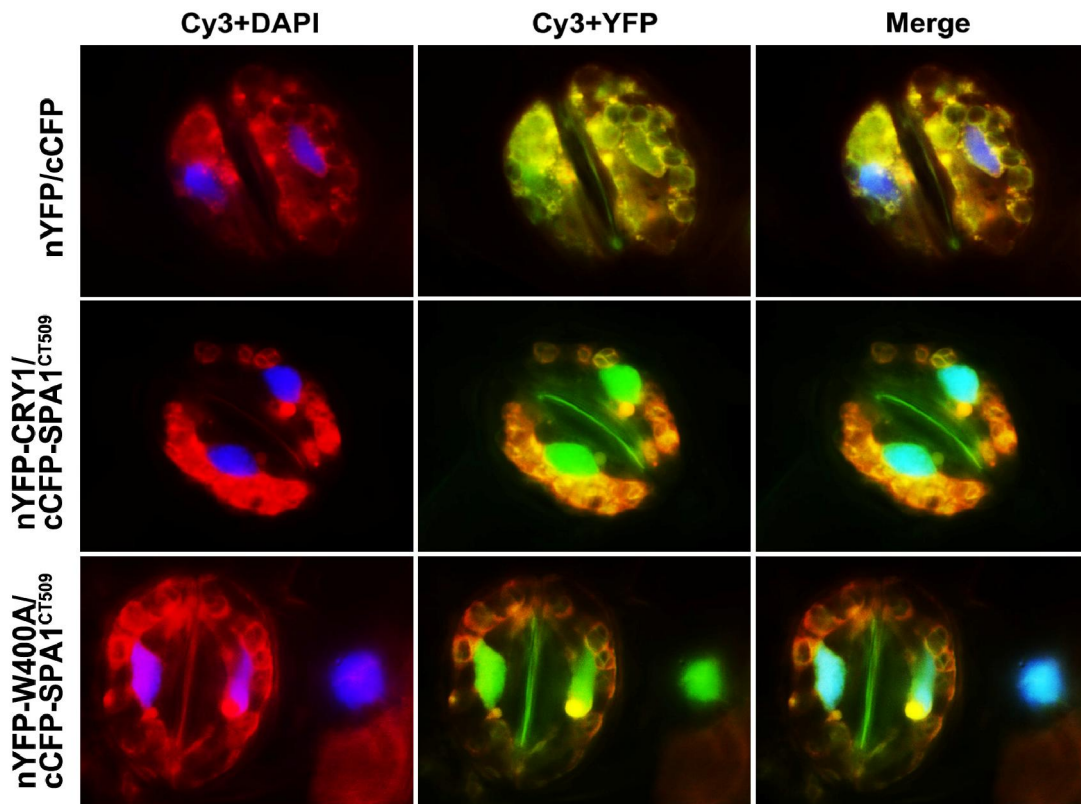
Fig.S13. BiFC assay showing interaction between CRY1^W-to-A mutants and the CRY1-interacting protein SPA1^CT509.

Three-week-old *Nicotiana benthamiana* plants grown in long-day (LD, 16h Light/8h Dark) were co-transformed with Agrobacterial strains harboring the plasmids encoding nYFP-CRY1 or nYFP-CRY1^W400A mutants and cCFP-SPA1^CT509. The plants were incubated for 12 h in the darkness after infection, transferred to white light for 48-72 h, and analyzed by the fluorescence microscopy. Images were taken by a camera at 100×magnification, the overlay of Cy3 autofluorescence (red) and DAPI (4',6-diamidino-2-phenylindole) nuclear signal (blue), and the overlay of Cy3 (Red) and YFP BiFC signal (green) of guard cells are shown.

Fig. S14

Fig.S14. BiFC assay showing interaction between CRY1^{W-to-A} mutants and the CRY1-interacting protein SPA1^{CT509}.

BiFC images of CRY1-SPA1^{CT509} (A), W400A-SPA1^{CT509} (B), W324A-SPA1^{CT509} (C), W377A-SPA1^{CT509} (D), W334A-SPA1^{CT509} (E) and W356A-SPA1^{CT509} (F) in *Nicotiana benthamiana*. The Co-transformation was performed as described in Fig.4. Images were taken by a camera at 10×magnification, The DAPI (4',6-diamidino-2-phenylindole) nuclear signal (blue), the YFP BiFC signal (green) and merge images are shown.

19